US011635394B2

(12) **United States Patent**
Ma et al.

(10) **Patent No.: US 11,635,394 B2**
(45) **Date of Patent: Apr. 25, 2023**

(54) **SENSING USING INVERSE MULTIPLE SCATTERING WITH PHASELESS MEASUREMENTS**

(71) Applicant: **Mitsubishi Electric Research Laboratories, Inc.**, Cambridge, MA (US)

(72) Inventors: **Yanting Ma**, Allston, MA (US); **Muhammad Asad Lodhi**, Edison, NJ (US); **Hassan Mansour**, Boston, MA (US); **Petros Boufounos**, Winchester, MA (US); **Dehong Liu**, Lexington, MA (US)

(73) Assignee: **Mitsubishi Electric Research Laboratories, Inc.**, Cambridge, MA (US)

(*) Notice: Subject to any disclaimer, the term of this patent is extended or adjusted under 35 U.S.C. 154(b) by 541 days.

(21) Appl. No.: **16/786,107**

(22) Filed: **Feb. 10, 2020**

(65) **Prior Publication Data**

US 2021/0247333 A1 Aug. 12, 2021

(51) **Int. Cl.**
G01N 23/20 (2018.01)
G01M 5/00 (2006.01)
(Continued)

(52) **U.S. Cl.**
CPC ***G01N 23/20*** (2013.01); ***G01M 5/0025*** (2013.01); ***G01N 22/00*** (2013.01); ***G01S 13/887*** (2013.01);
(Continued)

(58) **Field of Classification Search**
None
See application file for complete search history.

(56) **References Cited**

U.S. PATENT DOCUMENTS

4,662,222 A * 5/1987 Johnson G01S 15/895 73/602
5,588,032 A * 12/1996 Johnson G01S 13/89 378/90

(Continued)

OTHER PUBLICATIONS

V. A. Mikhnev and P. Vainikainen, "Two-step inverse scattering method for one-dimensional permittivity profiles," in IEEE Transactions on Antennas and Propagation, vol. 48, No. 2, pp. 293-298, Feb. 2000, doi: 10.1109/8.833079. (Year: 2000).*

(Continued)

Primary Examiner — Bernarr E Gregory
(74) *Attorney, Agent, or Firm* — Gennadiy Vinokur; Hironori Tsukamoto

(57) **ABSTRACT**

A permittivity sensor, for determining an image of a distribution of permittivity of a material of an object in a scene, comprising an input interface, a hardware processor, and an output interface is provided. The input interface is configured to accept phaseless measurements of propagation of a known incident field through the scene and scattered by the material of the object in the scene. The hardware processor is configured to solve a multi-variable minimization problem over unknown phases of the phaseless measurements and unknown image of the permittivity of the material of the object by minimizing a difference of a nonlinear function of the known incident field and the unknown image with a product of known magnitudes of the phaseless measurements and the unknown phases. Further, the output interface is configured to render the permittivity of the material of the object provided by the solution of the multi-variable minimization problem.

13 Claims, 11 Drawing Sheets

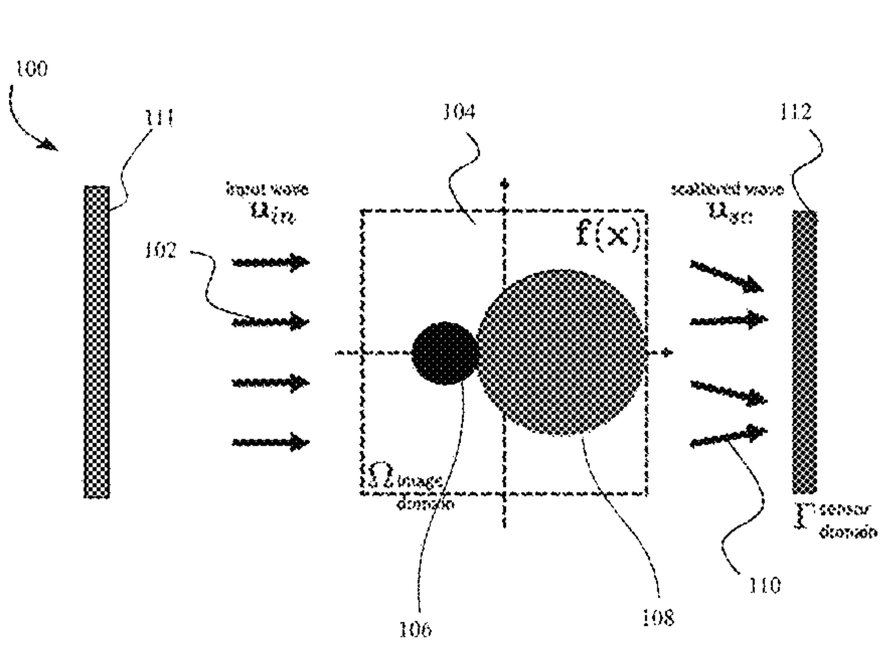

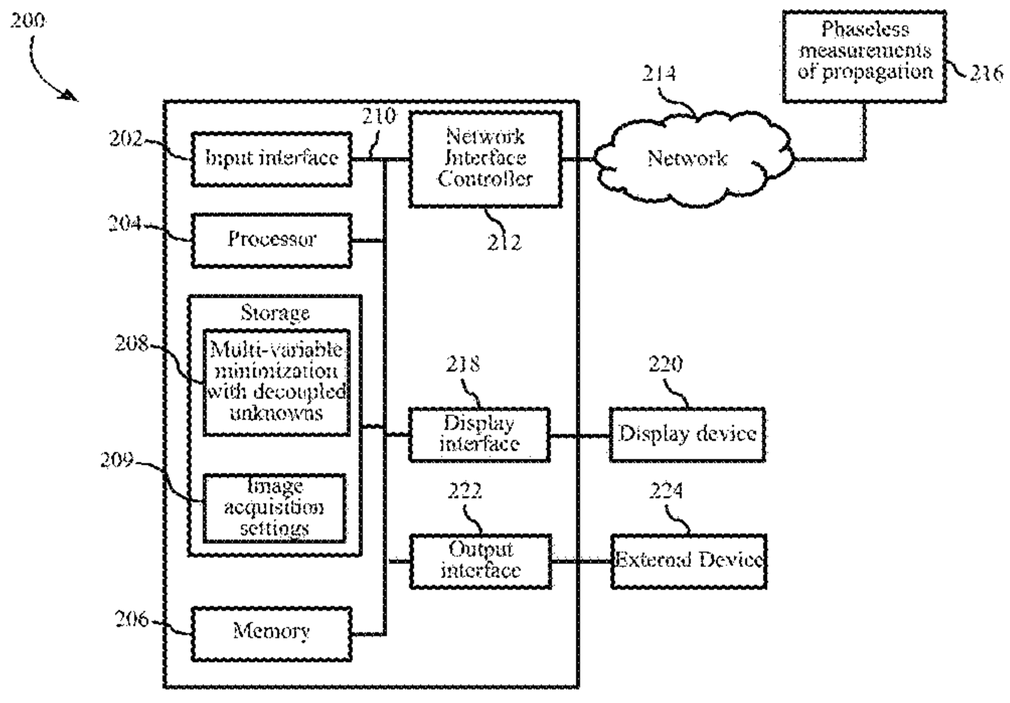

(51) **Int. Cl.**

G01N 22/00	(2006.01)
G01S 13/88	(2006.01)
G01S 13/89	(2006.01)
G01V 8/00	(2006.01)
G01V 9/00	(2006.01)
G01S 13/00	(2006.01)

(52) **U.S. Cl.**
CPC ***G01S 13/89*** (2013.01); ***G01V 8/00*** (2013.01); ***G01V 9/00*** (2013.01); *G01N 2223/101* (2013.01); *G01N 2223/405* (2013.01)

(56) **References Cited**

U.S. PATENT DOCUMENTS

9,329,263	B2 *	5/2016	Haynes	G01S 13/89
9,519,054	B2 *	12/2016	Kim	G01S 13/88
10,768,214	B2 *	9/2020	Safavi-Naeini	G01N 22/00
10,976,461	B2 *	4/2021	Arumugam	G01S 13/885

OTHER PUBLICATIONS

J. Fessler. Apr. 17, 2019,18:24 (class version). Chapter 6. Alternating minimization. Alternating minimization fessler/course/598.

Pham et al. Versatile reconstruction framework for diffraction tomography with intensity measurements and multiple scattering. Optics express 2749, Research Article. vol. 26, No. 3. Feb. 5, 2019.

* cited by examiner

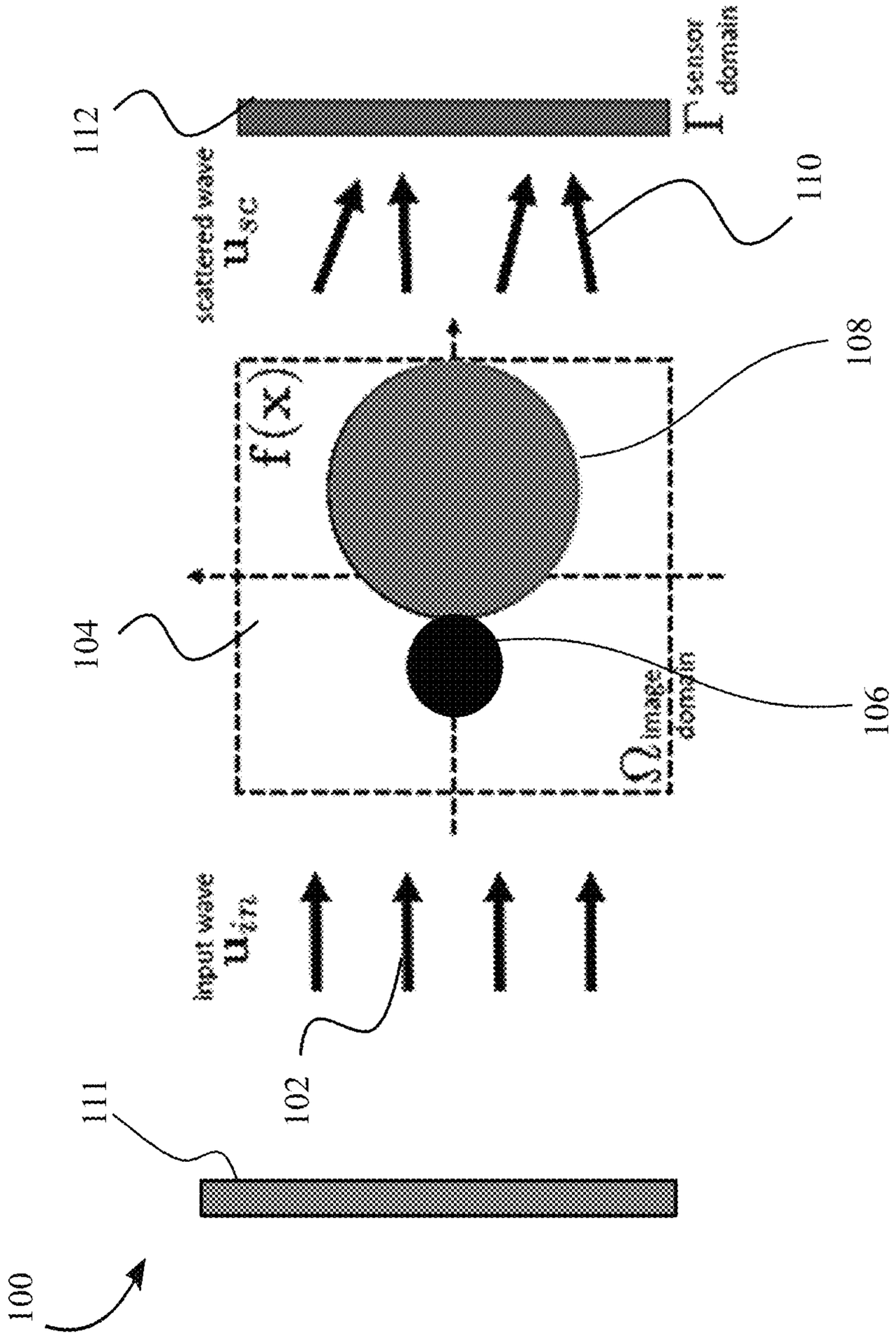
100
102
111
sensor domain
112
scattered wave u_{sc}
110
108
$f(x)$
104
106
$\Omega_{image\ domain}$
input wave u_{in}

FIG. 1

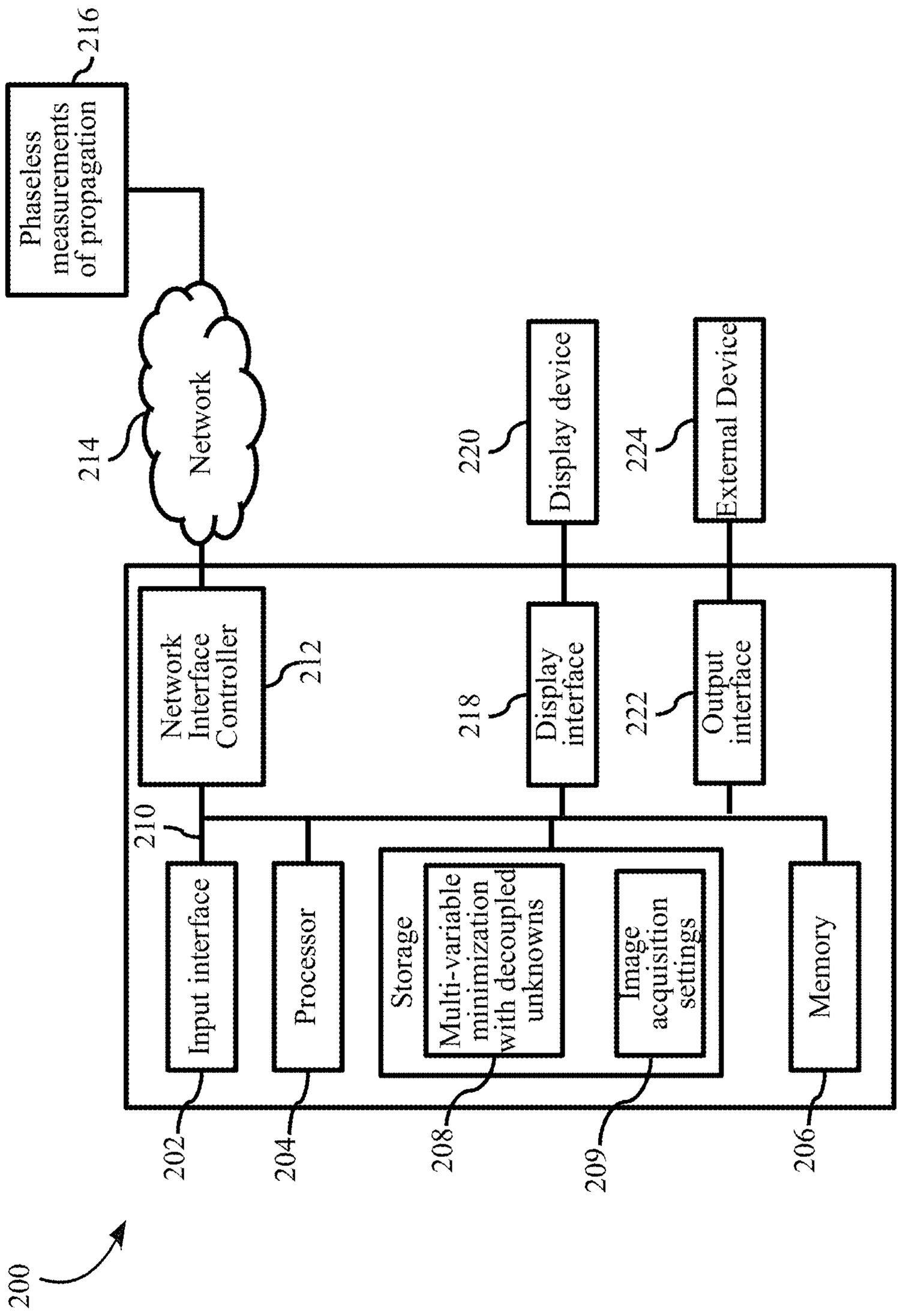
200
202
Input interface
204
Processor
206
Memory
208
Multi-variable minimization with decoupled unknowns
209
Image acquisition settings
210
Storage
212
Network Interface Controller
214
Network
216
Phaseless measurements of propagation
218
Display interface
220
Display device
222
Output interface
224
External Device

FIG. 2A

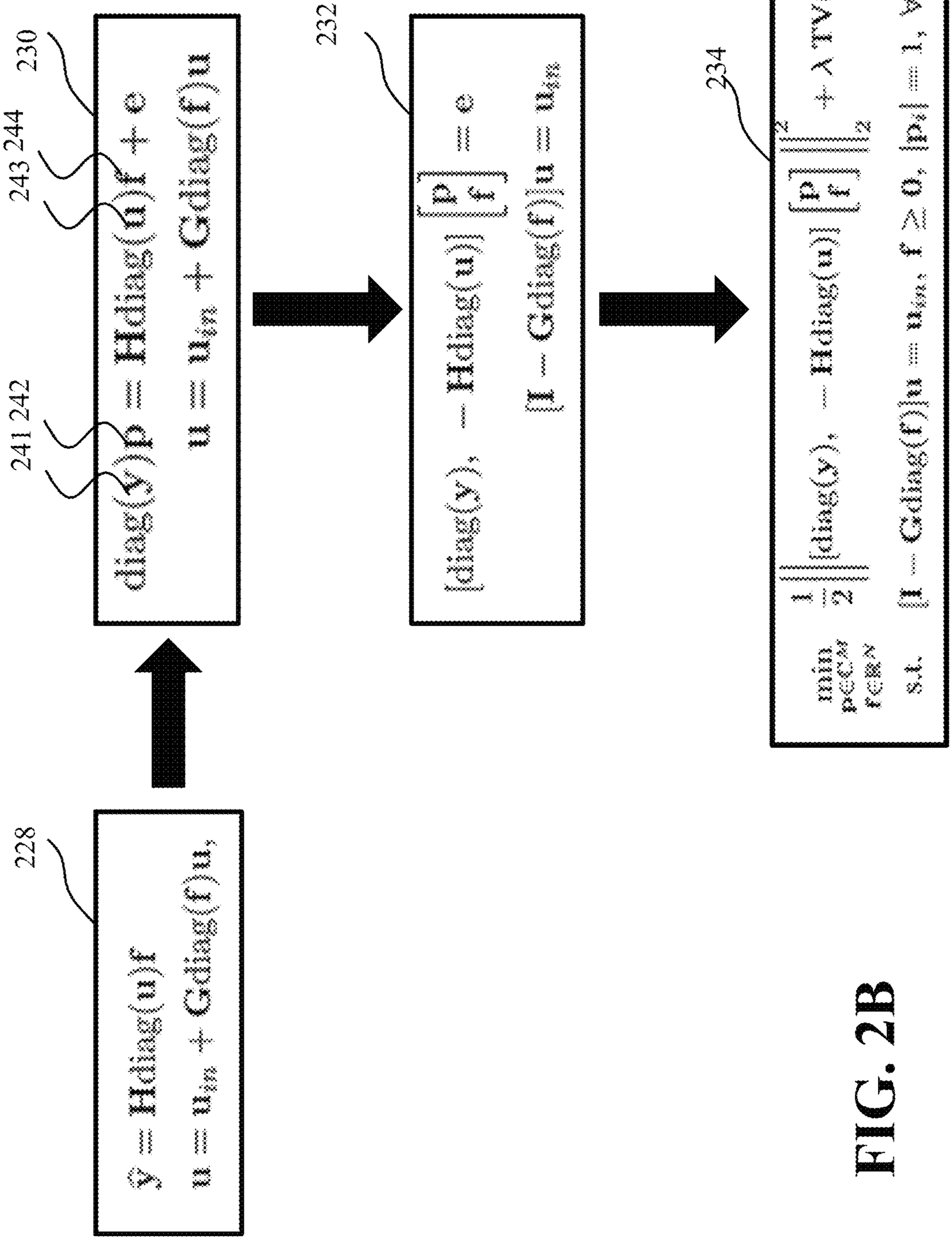
228
y = Hdiag(u)f
u = u_in + Gdiag(f)u,
241 242
diag(y)p = Hdiag(u)f + e
u = u_in + Gdiag(f)u
243 244
230
232
[diag(y), −Hdiag(u)] [p; f] = e
[I − Gdiag(f)]u = u_in
234
min_{p∈ℝ^n, f∈ℝ^m} 1/2 ||[diag(y), −Hdiag(u)] [p; f]||_2^2 + λ TV(f)
s.t. [I − Gdiag(f)]u = u_in, f ≥ 0, |p_i| = 1, ∀i.

FIG. 2B

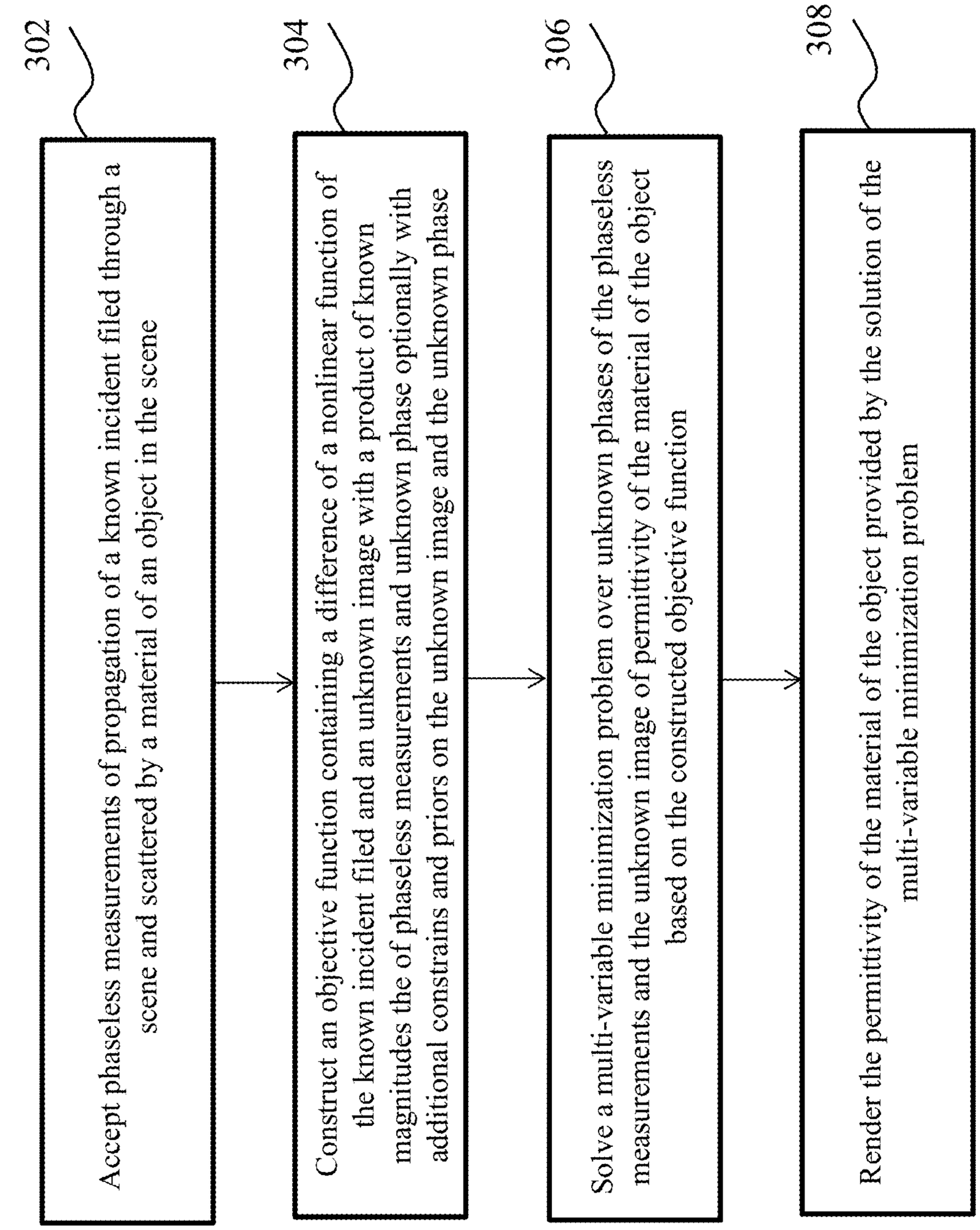
300
302
Accept phaseless measurements of propagation of a known incident filed through a scene and scattered by a material of an object in the scene
304
Construct an objective function containing a difference of a nonlinear function of the known incident filed and an unknown image with a product of known magnitudes the object of phaseless measurements and unknown phase optionally with additional constrains and priors on the unknown image and the unknown phase
306
Solve a multi-variable minimization problem over unknown phases of the phaseless measurements and the unknown image of permittivity of the material of the object based on the constructed objective function
308
Render the permittivity of the material of the object provided by the solution of the multi-variable minimization problem

FIG. 3

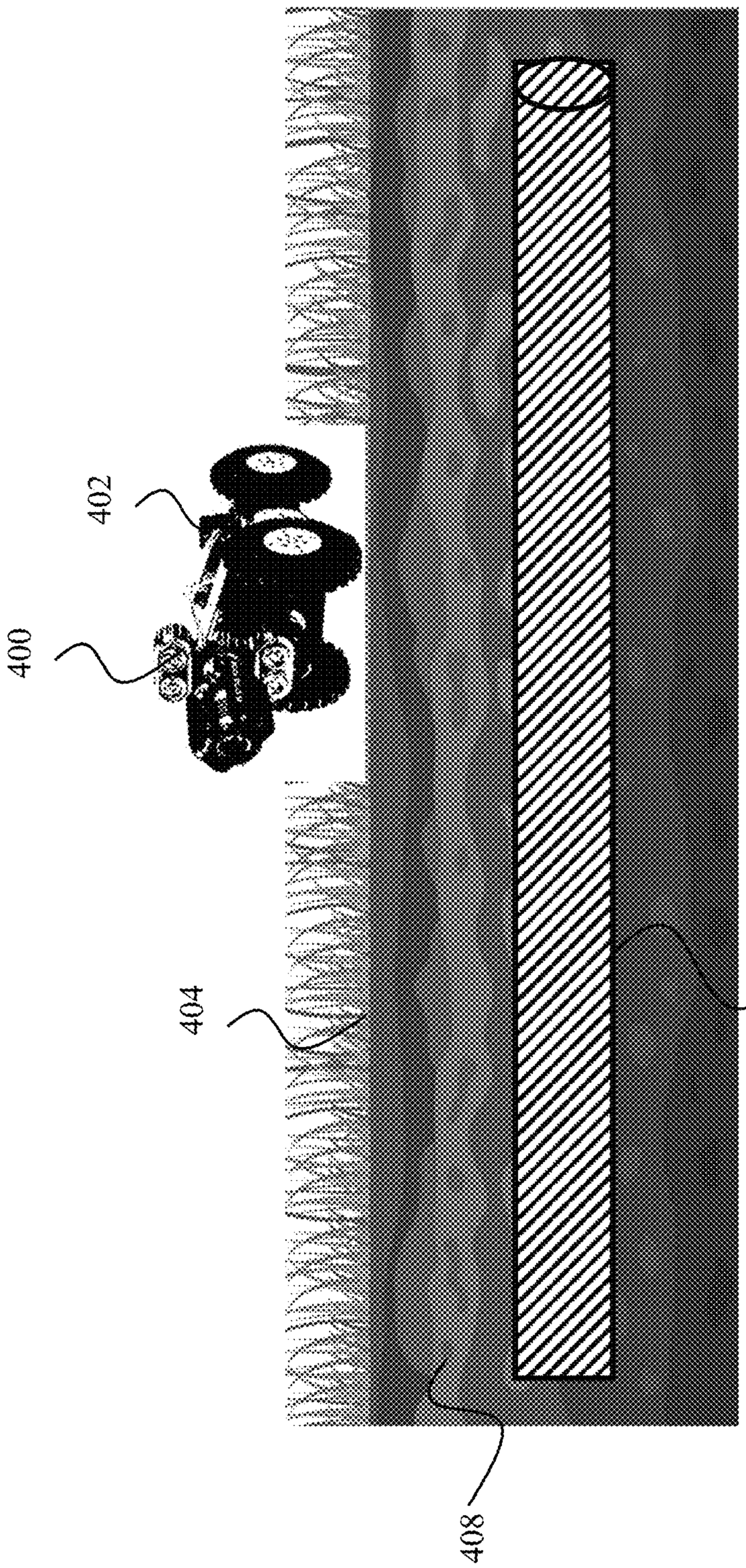

FIG. 4A

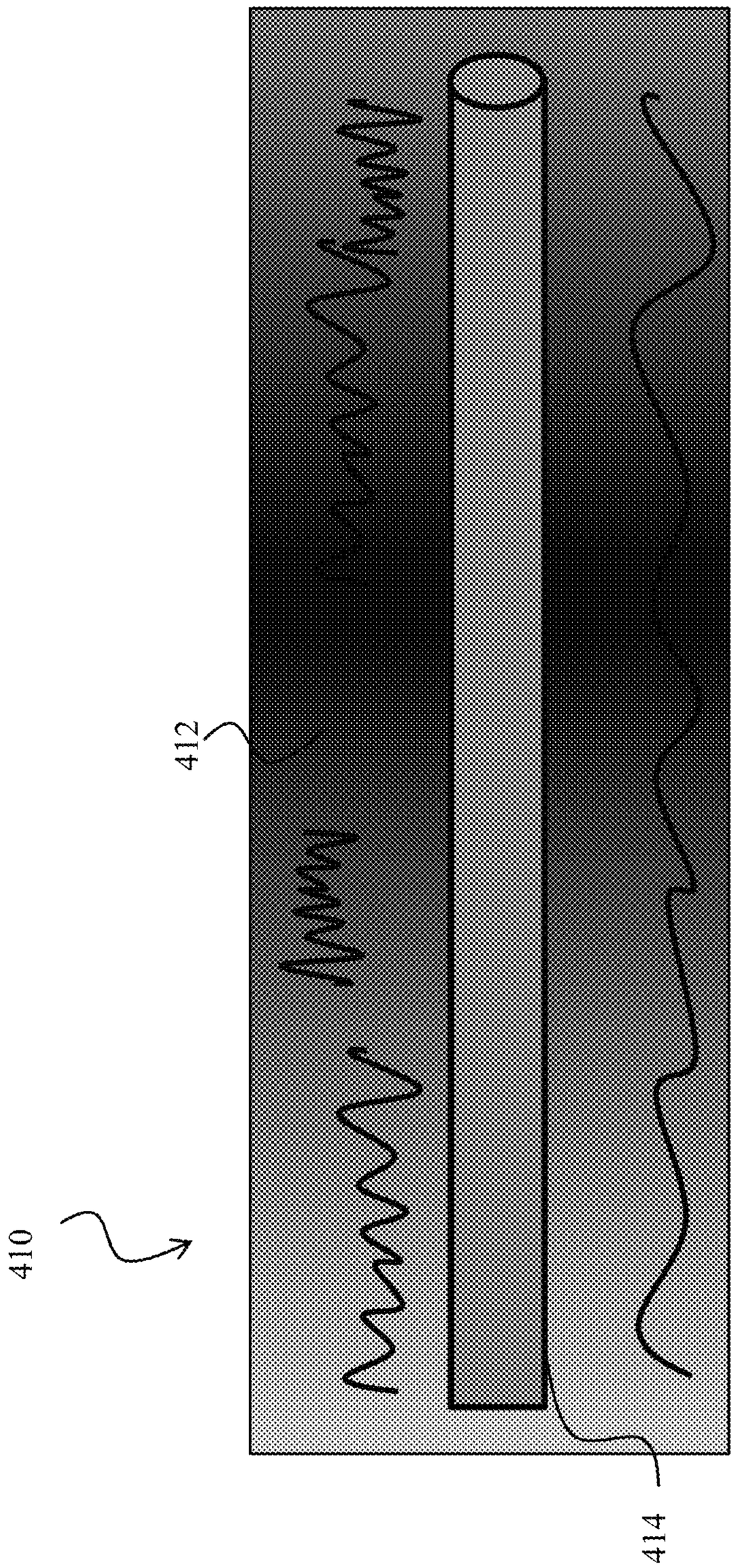

FIG. 4B

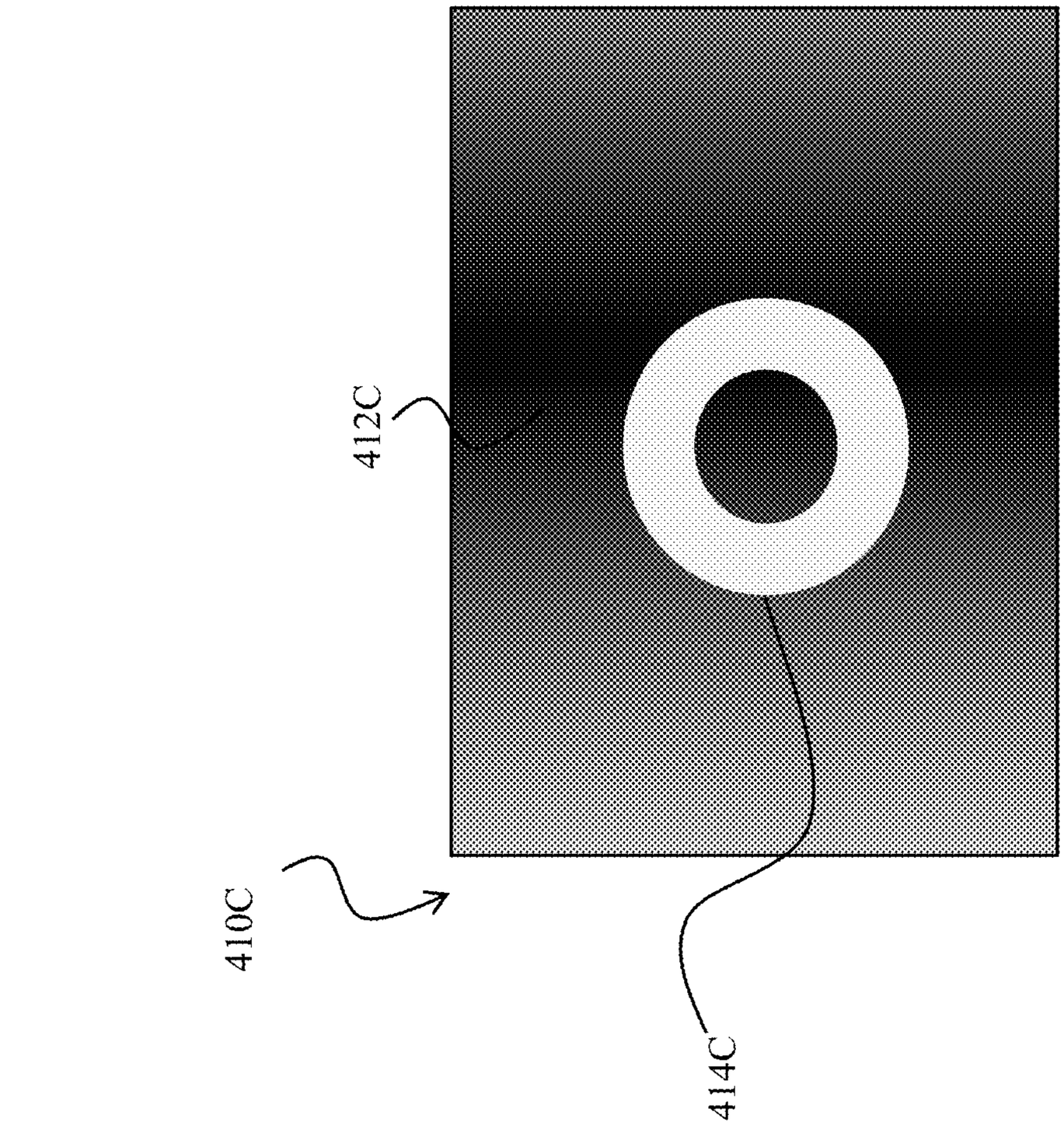

FIG. 4C

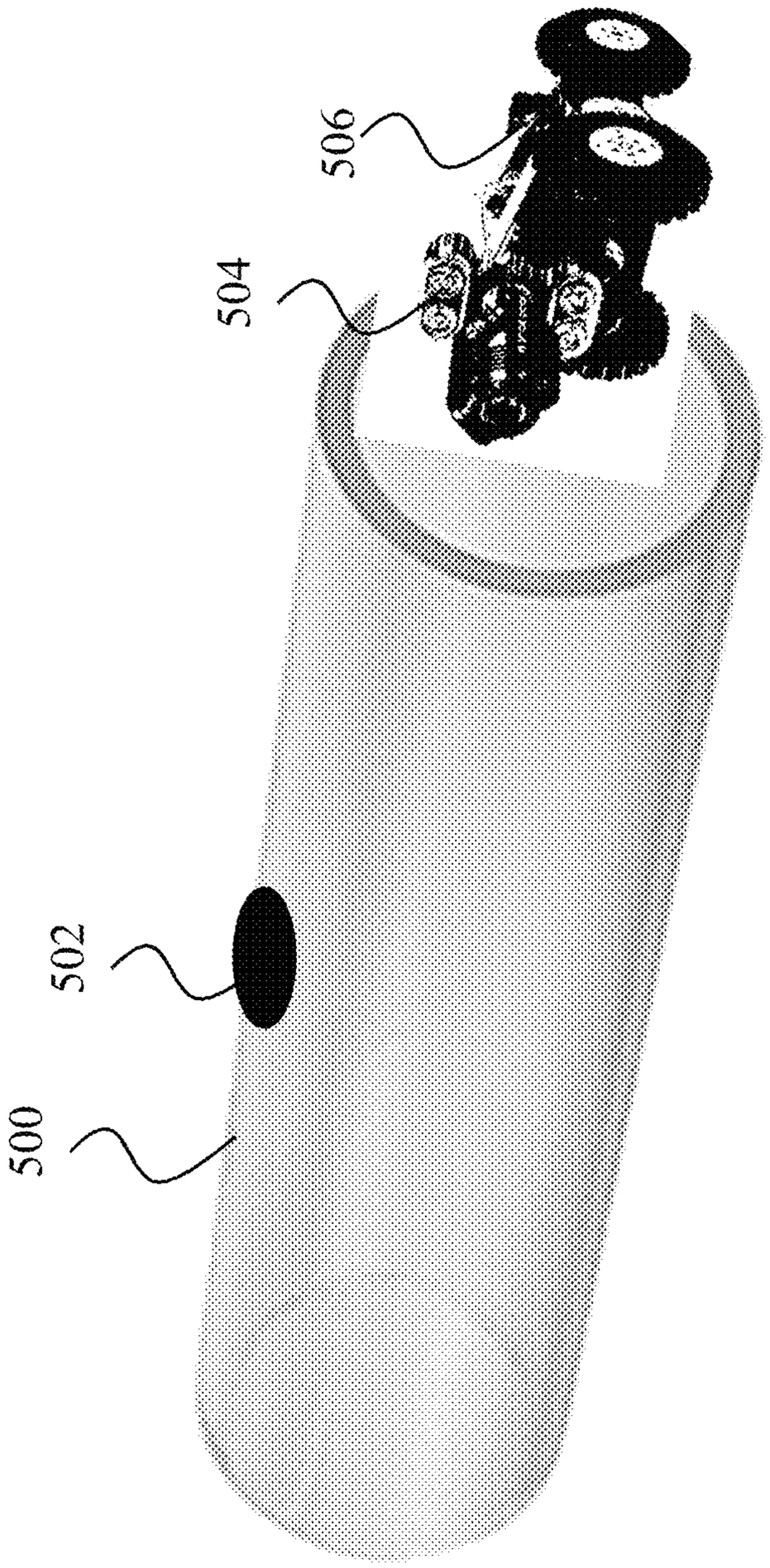

FIG. 5A

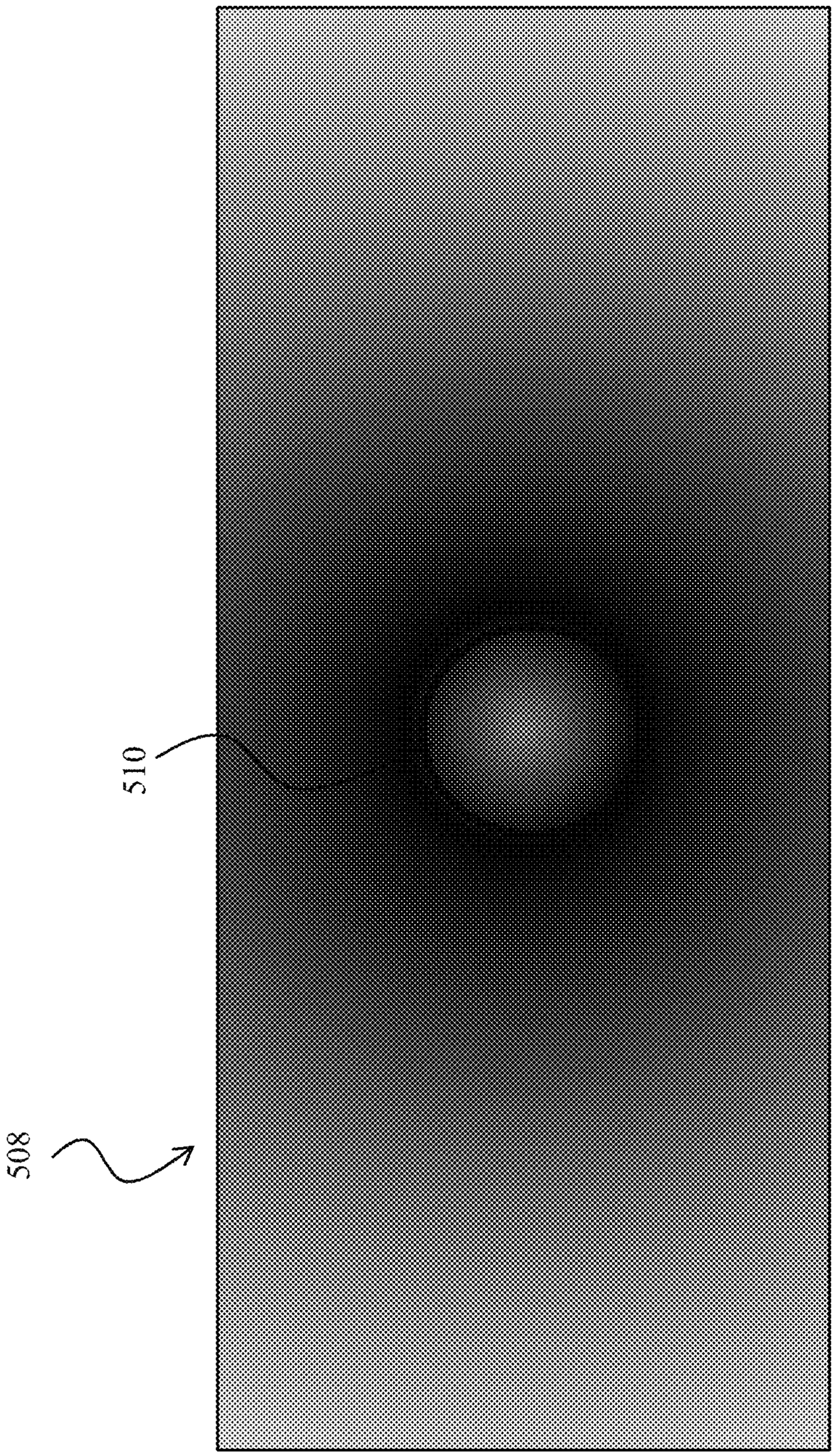

FIG.5B

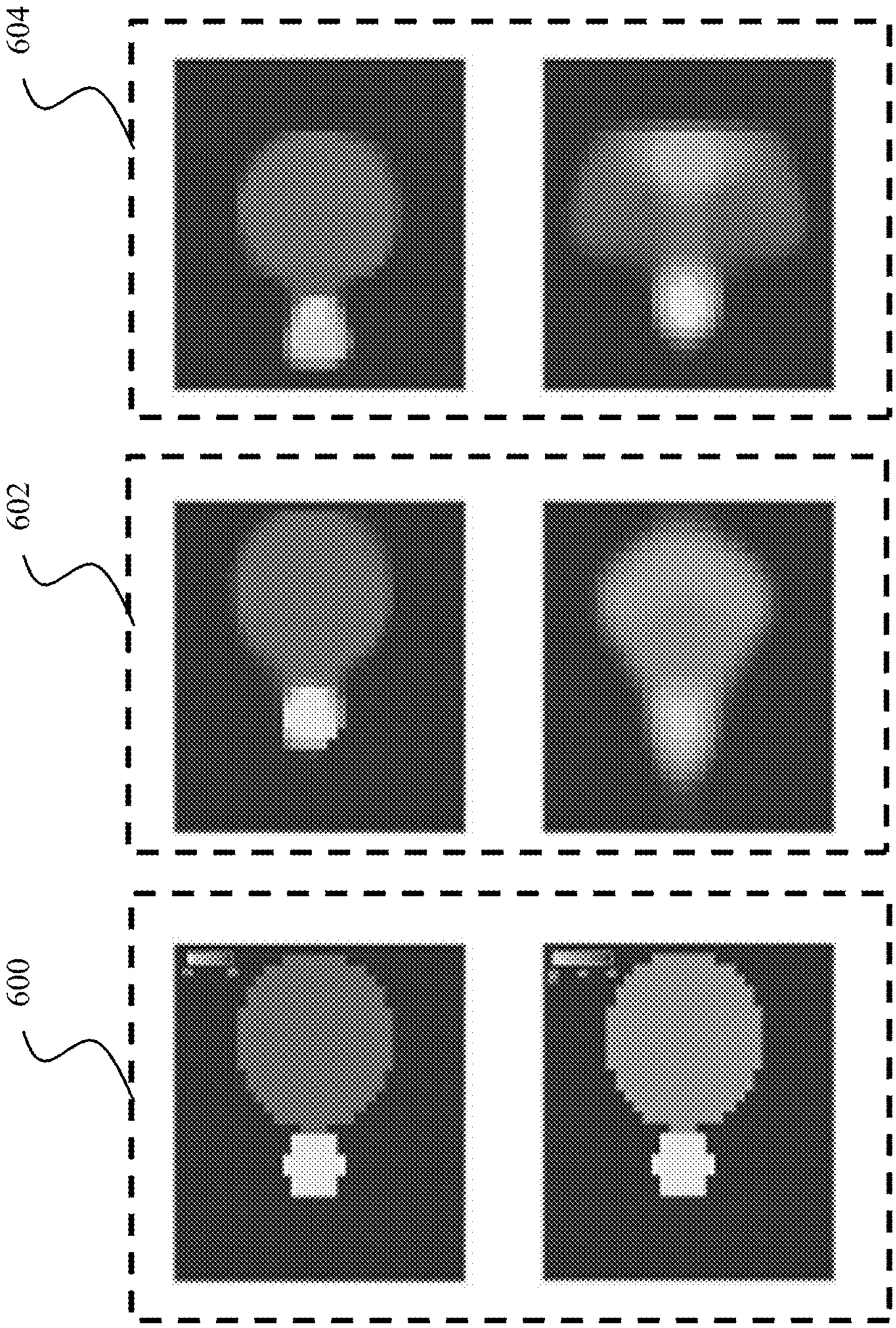

FIG. 6

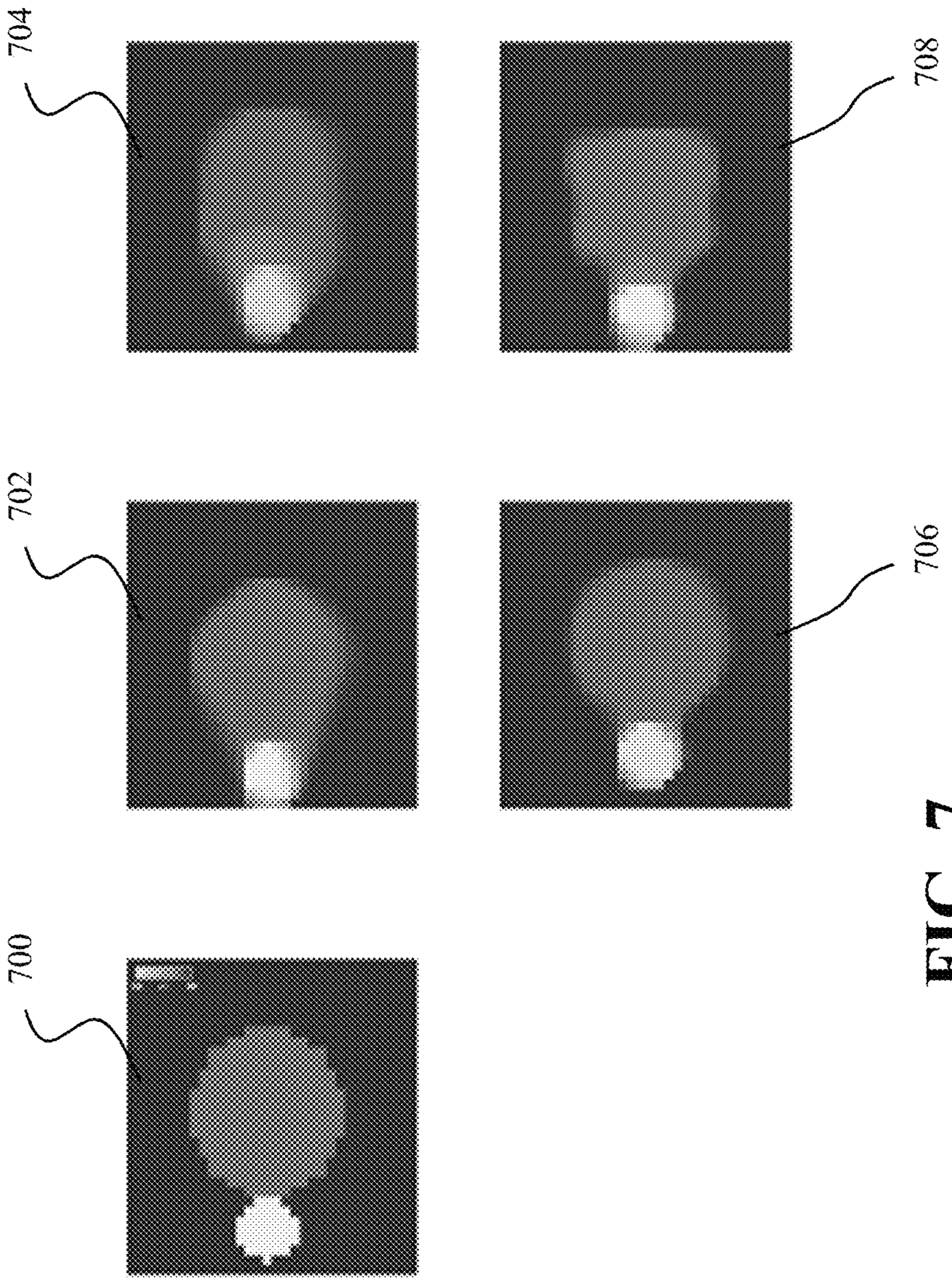

FIG. 7

SENSING USING INVERSE MULTIPLE SCATTERING WITH PHASELESS MEASUREMENTS

TECHNICAL FIELD

This invention relates to sensing systems and methods, and more specifically to system and method for determining an image of a distribution of permittivity of a material from phaseless (intensity-only) measurements of its scattered electromagnetic field.

BACKGROUND

The composition or internal structure of an object can be visualized by numerically generating an image that represents distribution of permittivity of the materials in the object. A transmitter emits a signal in some modality, such as an electromagnetic (EM), light or ultrasonic wave or pulse, which propagates through the object, reflects off various structures inside the object, and propagates to a receiver sensor array. In particular, the non-uniform distribution of the permittivity inside the object, due to changes in its material composition and structure, forces the wave or the pulse to deviate from a straight-line trajectory and scatter in different paths. Part of the scattered signal is measured by sensors placed inside or around the object. Inverse scattering is the problem of reconstructing the permittivity distribution inside the object from the measured scattered wave or pulse. The composition of the object can also be visualized by numerically generating an image that represents this distribution of the permittivity of the materials in the object.

Depending on the material composition of the object, the received signal often results from the multiple reflections of the propagating pulse due to multiple scattering from the structures in the object, which results in artifacts that clutter the reconstructed image. Most of the conventional methods addressing this problem have considered linear forward models that enable an efficient convex formulation of inverse problem by neglecting the multiple scattering. However, these linear models tend to be highly inaccurate in high contrast settings, i.e., when the permittivity changes significantly between different structures in the object and the background. This effect is especially prominent in situations where the size of the structure is large with respect to the wavelength of the incident wave.

To address this deficiency, some methods use nonlinear formulation of image acquisitions that provide a more accurate representation of the physical setup by modeling multiple scattering and facilitate imaging in high contrast settings. These nonlinear inverse problems are usually more challenging to solve than solving their linear counterparts. Still, several methods have been recently developed to directly invert the nonlinear forward model, hence enabling imaging in high permittivity contrast settings, provided that both the magnitude and the phase of the scattered wave are available.

However, in a number of applications, measuring phase of the scattered wave can be impractical or expensive. In others, the phase measurements can be very noisy or unreliable. In these applications, the problem becomes one of phaseless image recovery, i.e., recovery from measurements lacking phase information of the measured scattered wave.

The common method for solving a phaseless image recovery problem is alternating minimization, i.e., methods that alternate between phase estimation (using phase retrieval techniques) and the inversion problem (based on the estimated phase). However, the alternating minimization is sensitive to the choice of optimization parameters. Some other methods, not based on alternating minimization, are less effective for practical imaging problems. Some methods exploit a good initialization or initial guess to determine a solution. However, it is difficult to provide the initial good initialization of the phaseless image recovery problem. Other methods lift the phaseless image recovery problem into a different domain (i.e. a higher dimensional domain) to solve the problem in that domain. However, solving the problem in a lifted higher dimensional space can be computationally prohibitive and can make incorporating image priors impractical.

Accordingly, there is a need for a method for reconstructing an object from phaseless measurements in the context of inverse multiple scattering.

SUMMARY

Some embodiments are based on recognition of the cause of the difficulties in solving phaseless image recovery problem. In solving this problem, the permittivity distribution of the materials in the measured object is the unknown image to be reconstructed. In the presence of phase information, a typical image reconstruction approach attempts to explain the acquired data as a function of the image being measured. This function is formulated based on the physical principles of wave propagation appropriate for the domain and modality of the application and is referred to as the forward model. Accordingly, the image reconstruction methods determine the unknown image of a scene that explains the measured data through this forward model. Naturally, when the measured data lack phase, the phaseless image reconstruction methods tend to adapt existing formulations of image recovery problem by inserting an unknown phase to correct the function of the image, such that the existing formulations can be reused. This approach, however, results in a multiplicative coupling between the unknown phase and the unknown image.

Some embodiments are based on realization that the multiplicative coupling between the unknown phase and the unknown image exacerbate non-convexity of image recovery problem, especially in the presence of nonlinearities due to multiple scattering and high contrast ratios. For this reason, there is a tendency to use alternating minimization, which is very sensitive to the choice of initialization and is prone to converge to undesirable local minima, which do not provide high quality reconstruction. In the case of linear forward models, it is possible to lift the image reconstruction problem to a higher dimensional space, making the resulting problem convex and eliminating phase as an unknown. However, this results in a prohibitively large optimization problem. Furthermore, in the nonlinear case of multiple scattering, the problem is still non-convex.

Accordingly, it is an object of some embodiments to decouple variables that represent the unknown image and the unknown phase in the forward model capturing image acquisition. Such a decoupling can enable the embodiments to solve the reconstruction problem over both unknowns simultaneously, e.g., with appropriate regularization for each.

Specifically, some embodiments are based on realization that the unknown phase can be incorporated in the image reconstruction problem by multiplying and correcting known phaseless measurements, such that the measurements incorporating phase can be explained by the image through the forward model. To that end, the phaseless measurements

are obtained by a measurement system, where the measurement system can be modelled as obtained by acquiring a magnitude value (i.e. the known phaseless measurement) of a complex non-linear measurement of the unknown image. Using this realization, the unknown phase is used to multiplicatively correct known parameters, i.e., the phaseless measurements. This is in contrast to previous formulations that attempt to recover a phase that multiplicatively modifies the forward model to explain the phaseless measurement. Thus, in the previous formulation, the unknown phase multiplies a function of the unknown image, i.e., there is multiplicative coupling of the unknowns. In contrast, the formulation of the embodiments decouples the unknown phase from the unknown image by coupling the unknown phase with known measurements.

However, the resulting problem is still nonlinear and non-convex because of the nonlinearity of the forward model under multiple scattering. This nonlinearity is due to the interdependence of the unknown image and a total field created by the propagation of the wave through the object and the interaction of the wave with the material structure of the object.

Some embodiments are based on another realization that the nonlinearity of the image acquisition can be modelled by representing the total field of wave propagation using the known incident field generated by the transmitters and the scattered field, scattered by the object in the unknown image. This realization allows representing a product of the phaseless measurements with the unknown phase as a nonlinear function of known incident field and unknown image of the object.

Such a formulation is still nonlinear and non-convex. However, the nature of this formulation leads to a better-behaved non-convex objective function (a function of the unknown image and the unknown phase) due to decoupling the multiplicative relationship between the unknown image and the unknown phase, and, therefore, allows for various non-convex and even convex solvers to obtain high quality reconstructed images. For example, some embodiments solve the phaseless image recovery problem by minimizing an objective function that includes a sum of a data fidelity term and a regularization term, where the data fidelity term is the difference between a nonlinear function of the known incident field and the unknown image of the scene and a product of the phaseless measurements with the unknown phase, and the regularization term includes a sum of a total variation penalty of the unknown image and a magnitude constraint of the unknown phase, for example that a valid phase variable has magnitude equal to one. In various implementations, the embodiments use convex and/or non-convex solvers to minimize the objective function using alternating minimization methods or simultaneous multi-variable minimization methods that solve the optimization over both unknowns simultaneously by updating both unknowns for each iteration. Examples of simultaneous multi-variable minimization methods include proximal gradient methods such as fast iterative shrinkage-thresholding algorithm (FISTA) and its variates. In particular, some embodiments use FISTA to minimize the aforementioned objective function and call the resulting algorithm phaseless iterative shrinkage-thresholding algorithm (PISTA). In some situations, the simultaneous multi-variable minimization methods show superior results over the alternating minimization methods.

In some embodiments, the measurement system is implemented in a civil infrastructure system that solves the phaseless image recovery problem by using the convex and/or non-convex solvers in order to detect at least one of defects of a material of an object, cavities, non-visible objects of a civil infrastructure (e.g., underground objects, pipe leaks or cavities under a road, or defects inside a bridge structure), any three-dimensional object in a three-dimensional space. In some implementations, the civil infrastructure system is a moving platform that moves within the civil infrastructure to detect at least one of defects of the material of the object, the cavities or the non-visible objects of the civil infrastructure. For example, the system might include a vehicle driving around, surveying the infrastructure.

Accordingly, one embodiment discloses a permittivity sensor for determining an image of a distribution of permittivity of a material of an object in a scene. The permittivity sensor includes an input interface configured to accept phaseless measurements of propagation of a known incident field through the scene and scattered by the material of the object in the scene; a hardware processor configured to solve a multi-variable minimization problem over unknown phases of the phaseless measurements and unknown image of the permittivity of the material of the object by minimizing a difference of a nonlinear function of the known incident field and the unknown image with a product of known magnitudes of the phaseless measurements and the unknown phases; and an output interface configured to render the permittivity of the material of the object provided by the solution of the multi-variable minimization problem.

Some implementations also use regularization terms of the unknown image and the unknown phase to improve the convergence.

Another embodiment discloses a method for determining an image of a distribution of permittivity of a material of an object in a scene, comprising accepting phaseless measurements of propagation of a known incident field through the scene and scattered by the material of the object in the scene; solving a multi-variable minimization problem over unknown phases of the phaseless measurements and unknown image of the permittivity of the material of the object by minimizing a difference of a nonlinear function of the known incident field and the unknown image with a product of known magnitudes of the phaseless measurements and the unknown phases; and rendering the permittivity of the material of the object provided by the solution of the multi-variable minimization problem.

BRIEF DESCRIPTION OF THE DRAWINGS

The presently disclosed embodiments will be further explained with reference to the attached drawings. The drawings shown are not necessarily to scale, with emphasis instead generally being placed upon illustrating the principles of the presently disclosed embodiments.

FIG. **1** shows a schematic of a setup for inverse scattering, according to some embodiments.

FIG. **2**A shows a block diagram of a permittivity sensor for determining an image of a distribution of permittivity of a material of an object in a scene, according to some embodiments.

FIG. **2**B shows a determination of optimization algorithm based on the phaseless measurements of propagation, according to some embodiments.

FIG. **3** shows a schematic for workflow of determining the image of the distribution of permittivity of the material of the object in the scene, according to some embodiments.

FIG. **4**A shows a schematic of a civil infrastructure system to generate a map of non-visible objects in a civil infrastructure, according to some embodiments.

FIG. **4**B shows an exemplary output of the map of the non-visible objects, according to some embodiments.

FIG. **4**C shows an alternative exemplary output of the map of the non-visible objects, according to some embodiments.

FIG. **5**A shows a schematic of a civil infrastructure system to generate a map of cavities of non-visible objects in a civil infrastructure, according to some embodiments.

FIG. **5**B shows an exemplary output of the map of the cavities of the non-visible objects in the civil infrastructure, according to some embodiments.

FIG. **6** shows a schematic of comparison of experiment results for permittivity distribution of a material of an object using the PISTA algorithm and state of art algorithms with high contrast settings, according to some embodiments.

FIG. **7** shows a schematic of comparison of experiment results for permittivity distribution of a material of an object using the PISTA algorithm and state of art algorithms at different frequencies, according to some embodiments

DETAILED DESCRIPTION

In the following description, for purposes of explanation, numerous specific details are set forth in order to provide a thorough understanding of the present disclosure. It will be apparent, however, to one skilled in the art that the present disclosure may be practiced without these specific details. In other instances, apparatuses and methods are shown in block diagram form only in order to avoid obscuring the present disclosure.

As used in this specification and claims, the terms "for example," "for instance," and "such as," and the verbs "comprising," "having," "including," and their other verb forms, when used in conjunction with a listing of one or more components or other items, are each to be construed as open ended, meaning that that the listing is not to be considered as excluding other, additional components or items. The term "based on" means at least partially based on. Further, it is to be understood that the phraseology and terminology employed herein are for the purpose of the description and should not be regarded as limiting. Any heading utilized within this description is for convenience only and has no legal or limiting effect.

Solution Overview

FIG. **1** shows a schematic of a setup **100** for inverse scattering image reconstruction according to some embodiments. In FIG. **1**, there is shown an object **106**, **108** in a scene (i.e. a bounded domain Ω **104**) and sensors **112** positioned outside the bounded domain Ω **104**. The object **106**, **108**, collectively, may correspond to a two- or three-dimensional single entity having multiple sub-parts (e.g., a first part **106** and a second part **108**). Alternatively, the object **106**, **108** may correspond to a single part as a complete entity. There is further shown an input wave **102** incident on the object **106**,**108** and is further scattered (as a scattered wave **110**) from the object **106**,**108**. There is further shown that the scattered wave **110** is received by the sensor **112**. The wave **102** is emitted by a transmitter **111**. In this exemplar embodiment, the transmitters **111** and the sensors **112** are located on opposite sides of the objects **106**, **108**. In alternative implementations, the transmitters **111** and the sensor **112** are located on the same side of the objects **106**, **108**. In some embodiments the transmitters **111** and the sensors **112** might use the same physical device, operating in transmitting or receiving mode.

The inverse scattering image reconstruction according to some embodiments estimates spatial permittivity profile $\varepsilon(x)$ in the bounded domain Ω **104**, where $x\in\mathbb{R}^2$ represents spatial coordinates in the bounded domain Ω **104**. For example, one or more transmitters **111** transmit the incident wave **102** in some modality, such as an electromagnetic (EM), light or ultrasonic wave or pulse, which propagates through the object **106**,**108** and illuminate the object **106**, **108**. The input wave **102** incident on the object **106**, **108** represents input field u_{in} that is typically known and determined by the system design and the laws of wave propagation. The object **106**,**108** scatters the incident wave **102** inside and outside the domain Ω **104** and, consequently, a scattered field due to the scattered wave **110** is established and can be measured. In particular, the non-uniform distribution of permittivity inside the object **106**,**108** due to changes in its material composition and structure, forces the incident wave **102** to deviate from a straight-line trajectory and scatter in different paths. The scattered field is measured by the sensors **112**, as u_{sc}. The measured the scattered field u_{sc} from a single or a plurality of sensors, known as array of sensors, is used to reconstruct the image of the object **106**,**108**.

The reconstruction of the image of the object **106**,**108** from the scattered field u_{sc} is called as inverse scattering. Therefore, a system including such a sensor (i.e. the sensor **112** or the array of sensors) may also be called as a measurement and/or a sensing system.

In such a manner, a total field u in the imaging setup **100** is the sum of the two fields (i.e. input field u_{in} and the scattered field u_{sc}) such that

$$u=u_{in}+u_{sc}.$$

Further, relationship among the total field u, the input field u_{in}, and the scattering object **106**,**108** through the scalar Lippmann-Schwinger relationship can be expressed by an equation as given below:

$$u(x)=u_{in}(x)+\int_{\Omega}g(x-x')u(x')f(x')dx',\forall x\in\mathbb{R}^2,$$

where, $f(x)=k^2(\varepsilon(x)-\varepsilon_b)$ represents the scattering potential, ε_b represents the permittivity of the background, $k=\pi/\lambda$ is wavenumber in vacuum, and $g(x)=j/4H_0^{(1)}(k_b\|x\|)$ is the free-space Green's function in 2D, with $H_0^{(1)}$ representing the zero-order Hankel function of the first kind, $k_b=k\sqrt{\varepsilon_b}$ representing the background wavenumber, and $\|\bullet\|$ representing the Euclidean norm.

Further, a discretized system for the imaging setup **100** is formulated as:

$$\hat{y}=H\ \mathrm{diag}(u)f$$

$$u=u_{in}+G\ \mathrm{diag}(f)u, \tag{1}$$

where $f\in\mathbb{R}^N$, $u\in\mathbb{C}^N$, and $u_{in}\in\mathbb{C}^N$ are samples of f(x), u(x) and $u_{in}(x)$, respectively, obtained at N points in the domain Ω **104**. The diag(f) represents a diagonal matrix with f on its main diagonal, and $\hat{y}\in\mathbb{C}^M$ represents the scattered wave observed in the sensor domain Γ. In some embodiments, the N points in the domain are selected to be on a regular grid, with appropriately fine discretization. In different embodiments, the discretization accuracy is a design parameter and/or guided by a wavelength of the transmitted pulse, to ensure that objects or features of the objects are taken into account if they are sufficiently large to interact with the incident or the scattered wave.

Further, the matrix $H\in\mathbb{C}^{M\times N}$ in formulation (1) corresponds to a mapping from an image domain to sensor domain Γ, as defined by discretizing the continuous Green's function g(x−x') for $x\in\Gamma$ and $x'\in\Omega$. Similarly, the matrix

$G \in \mathbb{C}^{N \times N}$ is the mapping within the image domain, as defined by discretizing the Green's function g(x−x') for x, x'∈Ω.

Some embodiments are based on recognition that, in a number of applications, measuring phase of the scattered wave can be impractical or expensive. In others, the phase measurements can be very noisy or unreliable. In these applications, the problem becomes one of phaseless image recovery, i.e., recovery from measurements lacking phase information of the measured scattered wave. For example, the phaseless image recovery problem is applicable to optical sensing, such as Fourier ptychographic microscopy and optical diffraction tomography, due to the difficulties of nonlinear coherent measurements. The phaseless image recovery problem is also applicable in a motion related applications due to nonlinearity of distortion caused by the motion and in terahertz (THz) sensing due to difficulties of phase measurements with sufficient resolution.

To that end, in some embodiments, the measurement system is phaseless, i.e., only the magnitude of the scattered wave u_{sc} is recorded. Accordingly, the acquired data (in the absence of noise) may be expressed using the formulation (1) as:

$$y=|H \text{ diag}(u)f| \tag{1}$$

$$u=u_{in}+G \text{ diag}(f)u_{sc} \tag{2}$$

The formulation (2) corresponds to nonlinear and phaseless image reconstruction, where $y \in \mathbb{R}^{M}_{\geq 0}$ represents the magnitude of the scattered wave ŷ observed in the sensor domain Γ.

Some embodiments are based on recognition that the image reconstruction methods determine the unknown image of a scene that explains the measured data through this forward model. Naturally, when the measured data lack phase, the phaseless image reconstruction methods tend to adapt existing formulations of image recovery problem by inserting an unknown phase to correct the function of the image, such that the existing formulations can be reused. This approach, however, results in a multiplicative coupling between the unknown phase and the unknown image. That multiplicative coupling between the unknown phase and the unknown image exacerbate non-convexity of image recovery problem, especially in the presence of nonlinearities due to multiple scattering and high contrast ratios.

Accordingly, it is an object of some embodiments to decouple variables that represent the unknown image and the unknown phase in the forward model capturing image acquisition. Such a decoupling can enable the embodiments to solve the reconstruction problem over both unknowns simultaneously, with appropriate regularization for each.

Specifically, some embodiments are based on realization that the unknown phase can be incorporated in the image reconstruction problem by multiplying and correcting known phaseless measurements, such that the measurements incorporating phase can be explained by the image through the forward model. To that end, the phaseless measurements are obtained by a measurement system, where the measurement system can be modelled as obtained by acquiring a magnitude value (i.e. the known phaseless measurement) of a complex non-linear measurement of the unknown image. Using this realization, the unknown phase is used to multiplicatively correct known parameters, i.e., the phaseless measurements. This is in contrast to previous formulations that attempt to recover a phase that multiplicatively modifies the forward model to explain the phaseless measurement. Thus, in the previous formulation, the unknown phase multiplies a function of the unknown image, i.e., there is multiplicative coupling of the unknowns. In contrast, the formulation of the embodiments decouples the unknown phase from the unknown image by coupling the unknown phase with known measurements.

For example, the unknown phase of the scattered wave **110** is modeled through a complex phase-only vector $p \in \mathbb{C}^{M}$, i.e., ŷ=y⊙p, where ⊙ denotes element-wise product. Thus, phaseless observations satisfy y⊙p=H diag (f)u. In presence of noise, the formulation (2) can be expressed as:

$$\text{diag}(y)p=H \text{ diag}(u)f+e$$

$$u=u_{in}G \text{ diag}(f)u \tag{3}$$

where $e \in \mathbb{C}^{M}$ represents the noise.

Some embodiments are based on an objective of estimating an unknown object f and an unknown phase p by the phaseless observations and the incident field u_{in}, under the constraints that f is a piecewise constant and the unknown phase p is a phase-only vector.

However, the resulting problem is still nonlinear and non-convex because of the nonlinearity of the forward model under multiple scattering. This nonlinearity is due to the interdependence of the unknown image and a total field created by the propagation of the wave through the object and the interaction of the wave with the material structure of the object.

Some embodiments are based on another realization that the nonlinearity of the image acquisition can be modelled by representing the total field of wave propagation using the known incident field generated by the transmitter and the scattered field, scattered by the object in the unknown image. This realization allows representing a product of the phaseless measurements with the unknown phase as a nonlinear function of known incident field and unknown image of the scene.

To that end, some embodiments solve a multi-variable minimization problem over unknown phase of the phaseless measurements and unknown image of the permittivity of the material of the object **106**,**108** by minimizing a difference of a nonlinear function of the known incident field u_{in} and the unknown image with a product of known magnitudes of the phaseless measurements and the unknown phase. Some embodiments further include regularization terms for the unknown image and the unknown phase.

Such a formulation is still nonlinear and non-convex. However, the nature of this formulation leads to a better-behaved non-convex objective function (a function of the unknown image and the unknown phase) due to decoupling the multiplicative relationship between the unknown image and the unknown phase, and therefore allows for various non-convex and even convex solvers to obtain high quality reconstructed images. For instance, if the total field u is known, the formulation (3) becomes linear because the formulation decouples the unknown phase p from the unknown image f. Hence, for example, some embodiments solve the phaseless image recovery problem by minimizing an objective function that includes the sum of a data fidelity term and a regularization term, where the data fidelity term includes the difference between a nonlinear function of the known incident field and the unknown image of the scene and a product of the phaseless measurements with the unknown phase, and the regularization term includes the sum of a total variation penalty of the unknown image and a magnitude constraint of the unknown phase (a valid phase variable has magnitude equal to one).

In various implementations, the embodiments use convex and/or non-convex solvers to minimize the objective function using an alternating minimization methods or simultaneous multi-variable minimization methods that solve the optimization over both unknowns simultaneously by updating both unknowns for each iteration. Examples of simultaneous multi-variable minimization methods include proximal gradient methods such as fast iterative shrinkage-thresholding algorithm (FISTA) and its variates. In particular, some embodiments use FISTA to minimize the aforementioned objective function and call the resulting algorithm phaseless iterative shrinkage-thresholding algorithm (PISTA). In accordance with the solution of the multi-variable minimization problem, an image of the permittivity of the material of the object **106**,**108** is rendered.

System Overview

FIG. **2**A shows a block diagram of a permittivity sensor **200** for determining an image of a distribution of permittivity of a material of the object **106**, **108** in a scene, according to some embodiments. The permittivity sensor **200** includes an input interface **202** configured to accept phaseless measurements of propagation **216**, from a device, e.g., from the sensor **112**, for determining the image of the distribution of the permittivity of the material of the object **106**,**108**.

Further, the permittivity sensor **200** includes a network interface controller (NIC) **212** adapted to connect the permittivity sensor **200** through a bus **210** to a network **214**. Through the network **214**, either wirelessly or through wires, the permittivity sensor **200** may receive the phaseless measurements of propagation **216**. The system **200** stores image acquisition settings **209** used by multi-variable minimization **208** to reconstruct the image of the scene. The image acquisition settings can include settings used by a forward operator capturing specifics of the image acquisition, such as type and mutual arrangement of imaging equipment transmitting and receiving reflection of transmitted signals from one or more objects in the scene, type and frequency of the signals, optics of the imaging equipment, and position and motion of the imaging equipment.

The image acquisition settings **209** can define an input field u_{in}. Additionally or alternatively, the phaseless measurements of propagation **216** may include information of input field u_{in} corresponding to the incident wave **102** and characteristics of the scattered wave **110** such as known parameters of the scattered wave **110** for example, the magnitude of the scattered wave **110**, and the like.

The permittivity sensor **200** includes a memory **206** that stores instructions executable by a processor **204**. The processor **204** may be a hardware processor configured to execute the stored instructions in order to control operations of the permittivity sensor **200**. The processor **204** may be a single core processor, a multi-core processor, a graphics processing unit (GPU), a computing cluster, or any number of other configurations. The memory **206** may include random access memory (RAM), read only memory (ROM), flash memory, or any other suitable memory systems.

In some embodiments, the memory **206** may store programming instructions to execute multi-variable minimization with decoupled unknowns **208**. The solution of the multi-variable minimization **208** performs non-convex phaseless image reconstruction by decoupling the unknown phase and the unknown image f. More specifically, based on the execution of such programming instructions, the processor **204** is configured to solve the multi-variable minimization problem over the unknown phase of the phaseless measurements **216** and the unknown image f of the permittivity of the material of the object **106**,**108** by minimizing a difference of the nonlinear function of the known incident field u_{in} and the unknown image f with the product of known magnitudes of the phaseless measurements **216** and the unknown phases, possibly including regularization terms for the unknown image and the unknown phases.

In some embodiments, the processor **204** is configured to solve the multi-variable minimization problem **208** using a simultaneous multi-variable minimization over both unknowns simultaneously by updating the both unknowns for each iteration. Examples of simultaneous multi-variable minimization includes a multi-variable gradient descent that finds minimum of a function such that the optimization algorithm provides a solution of the inverse multiple scattering image reconstruction problem.

Accordingly, the memory can store a set of instructions for solving the multi-variable minimization problem **208**. Examples of such instructions include proximal gradient methods such as Phaseless Iterative Shrinkage-Thresholding Algorithm (PISTA) and the like to simultaneously update the unknown object (i.e. an image of the object **106**,**108**) and the unknown phase of the measurements (i.e. the scattered field **110**) at each iteration. Alternatively, the memory **206** may store a set of program instructions corresponding to alternating minimization algorithm and other algorithms capable of solving non-convex optimization problems.

In some implementations, the permittivity sensor **200** is connected to an output interface **222** through the bus **210** adapted to connect the permittivity sensor **200** to an external device **224** configured to render the distribution of the permittivity of the material of the object **106**,**108** output by the permittivity sensor **200**. In some other embodiments, the permittivity sensor **200** is communicatively coupled to a plurality of external devices.

Additionally, or alternatively, in one embodiment, the permittivity sensor **200** is connected to a display interface **218** through the bus **210** adapted to connect the permittivity sensor **200** to a display device **220**. The display device **220** is configured to render the result of the image inversion that corresponds to an image of the distribution of the permittivity of the material of the object **106**,**108** output by the permittivity sensor **200**.

Some embodiments are based on a realization that the object **106**,**108** is illuminated by the incident wave **102** transmitted from the one or more transmitters and further the incident wave **102** is scattered by the material of the object **106**,**108**. The incident wave **102** is selected prior to illuminate the object **106**,**108** based on a combination of various frequencies. Accordingly, the incident wave **102** is a known parameter and the incident field u_{in} is known.

Further, the processor **204** is configured to accept, via the input interface **202**, the phaseless measurements of propagation **216** of the known incident field u_{in} through a scene and scattered by the material of the object **106**,**108** present in the scene. The phaseless measurements of propagation **216** includes the information of the input field u_{in} corresponding to the incident wave **102** and the characteristics of the scattered wave **110** such as the known parameters of the scattered wave, for example the magnitude of the scattered wave **110**, and the like.

Based on the acceptance of the phaseless measurements of propagation **216**, the processor **204** is further configured to retrieve the set of program instructions stored in the memory **206** in order to solve a multi-variable minimization problem over the unknown phase of the phaseless measurements **216** and unknown image f of the permittivity of the material of the object **106**,**108**.

To that end, the processor **204** executes the retrieved set of program instructions to minimize an objective function that includes the difference of a nonlinear function of the known incident field u_{in} and the unknown image f with a product of known magnitudes of the phaseless measurements **216** and the unknown phases, possibly including regularization terms of the unknown image and the unknown phases. More specifically, the processor **204** executes the set of programming instructions based on the phaseless measurements of propagation **216** in order to minimize the objective function such that the multi-variable minimization problem is solved.

In some embodiments, the set of program instructions corresponding to the alternating minimization is executed by the processor **204**. Alternatively, the set of instructions corresponding to a multi-variable proximal gradient method is executed by the processor **204**. The multi-variable proximal gradient method is implemented using execution of algorithms such as PISTA.

By the solution of the multi-variable minimization problem, the processor **204** is configured to determine distribution of permittivity of the material of the object **106**,**108**. More specifically, the processor **204** determines an image of the distribution of the permittivity of the material of the object **106**,**108**. Further, the permittivity of the material of the object **106**,**108** is rendered on the external device **224** via the output interface **222**. Additionally, or alternatively, the permittivity of the material of the object **106**,**108** is rendered on the display device **218** via the display interface **220**.

By solving the multi-variable minimization problem over the unknown phases of the phaseless measurements **216** and the unknown image f, the processor **204** optimizes the unknown parameters given the magnitude of the scattered field u_{sc}. Accordingly, the permittivity sensor **200** facilitates accurate determination of the image of the distribution of the permittivity of the material of the object **106**,**108** based on optimization of the unknown parameters given the magnitude of the scattered field u_{sc}.

Exemplar Solutions

FIG. **2**B shows determination of optimization algorithm based on the phaseless measurements of propagation **216**, according to some embodiments.

It is an objective of some embodiments to decouple variables that represent the unknown image and the unknown phase in the forward model capturing image acquisition in order to optimize unknown parameters given the magnitude of the scattered field u_{sc} such that the reconstruction problem over both the unknown image and the unknown phase is solved simultaneously and the multiplicative coupling between the unknown image and the unknown phase is removed.

Referring to FIG. **1**, discretized system for the imaging setup **100** is formulated as the formulation (1) **228**, which is further rearranged based on the phaseless measurement system as the formulation (2) in the absence of noise. Further, the formulation (2) is expressed as the formulation (3) in the presence of noise **230**.

The formulation (3) removes the multiplicative coupling between the unknown phase and the unknown image fin the discretized system for the imaging setup **100**. Hence, the formulation (3) defines a multi-variable minimization problem over unknown phases of the phaseless measurements and unknown image of the permittivity of the material of the object that minimizes a difference of a nonlinear function of the known incident field **243** and the unknown image **244** with a product of known magnitudes **242** of the phaseless measurements and the unknown phases **242**;

By the rearrangement of the formulation (3), following expression **232** is obtained:

$$[\mathrm{diag}(y), -H\mathrm{diag}(u)]\begin{bmatrix} p \\ f \end{bmatrix} = e \tag{4}$$

$$[I - G\mathrm{diag}(f)]u = u_{in}, \tag{5}$$

where p and fin the formulation (4) lie in a null space of the matrix [diag(y), −H diag(u)] in the absence of noise, which may not be unique.

More specifically, p and the fin the formulation (4) in the null space includes the trivial all-zero solutions which leads to ambiguous results. This effect is called as the multi-variable minimization problem. Further, a constraint (5) on the total field u reduces the size of the solution space, and a set of constraints are introduced in order to further resolve such a problem.

To that end, some embodiments are based on a realization that object permittivity contrast f is typically smooth in spatial coordinates and the object permittivity contrast f is only associated with non-negative values. Additionally, p is a phase-only complex vector with unit entry-wise magnitudes such that $|p_i|=1$ for i=1, . . . , M. With these additional priors and constraints, some embodiments use total-variation(TV)-based regularization with a non-negativity constraint on the object permittivity contrast f and a unit-magnitude constraint on the phase-only vector p, thus the phaseless inverse scattering requires solving the following optimization **234**

$$\min_{\substack{p\in C^M \\ f\in \mathbb{R}^N}} \frac{1}{2}\left\|[\mathrm{diag}(y), -H\mathrm{diag}(u)]\begin{bmatrix} p \\ f \end{bmatrix}\right\|_2^2 + \lambda TV(f) \tag{6}$$

$$\text{s.t. } [I - G\mathrm{diag}(f)]u = u_{in},\ f \geq 0,\ |p_i| = 1,\ \forall\, i.$$

where,

$$TV(f) = \sum_{n=1}^{N} \sqrt{|D_1 f|^2 + |D_2 f|^2}$$

represents TV regularization,

D_i represents the discrete difference operator in the i-th spatial dimension, and

λ is the optimization parameter.

Writing u as a function f according to (5) and plugging it into the first term of (6), the first term of (6) is a differentiable function off and the gradient can be efficiently computed via a conjugate gradient method. Accordingly, the processor **204** may be configured to solve the multi-variable minimization problem using a proximal gradient method to perform simultaneous multi-variable minimization over both unknowns simultaneously by updating the both unknowns for each iteration. The gradient of the f and p is estimated recursively for a fixed number of iterations or until a termination condition is met. The termination condition may be based on simultaneous estimation of the gradient of the f and p until a unique value of the gradient is achieved.

To that end, the formulation (6) may be solved by use of a method (hereinafter "Algorithm 1") based on known phaseless measurements such as known incident field u_{in},

known magnitude of the phaseless measurements **216**. Such an algorithm is called as PISTA, which uses FISTA as the solver for the optimization problem (6). In some embodiments, the formulation (6) is solved based on FISTA. In some alternative embodiments, the formulation (6) is solved based on other algorithms that can solve non-convex and non-smooth optimization problems.

To that end, the processor **204** may be configured to execute the set of instructions corresponding to the PISTA algorithm to simultaneously recover the unknown object and the phase of the measurements from the nonlinear and nonconvex inverse scattering problem.

Algorithm 1: PISTA

Algorithm 1: PISTA - Phaseless Iterative Shrinkage-Thresholding Algorithm

Data: y, H, G, α, λ

$q_1 = f_0 = 0$; $s_1 = p_0 = 1$;

while stopping criteria do

$$k = k + 1;$$
$$f_k = \mathcal{P}_{TV,\lambda,(\cdot)\geq 0}(q_k - \alpha\nabla_f(q_k, s_k));$$
$$p_k = \mathcal{P}_{|\cdot|=1}(s_k - \alpha\nabla_p(q_k, s_k));$$
$$t_{k+1} = \frac{1+\sqrt{1+4t_k^2}}{2};$$
$$q_{k+1} = f_k + \frac{t_k - 1}{t_{k+1}}(f_k - f_{k-1});$$
$$s_{k+1} = p_k + \frac{t_k - 1}{t_{k+1}}(p_k - p_{k-1});$$

end

Result: $\hat{p}$, $\hat{f}$

In the Algorithm 1,

α represents a step size,

$P_{TV,\ \lambda,\ |\cdot|\geq 0}$ represents the proximal mapping for TV regularization with non-negativity constraints,

$P_{|\cdot|=1}$ represents the nonconvex proximal mapping on to the surface of the M-dimensional complex sphere, obtained by scaling each complex entry of a vector to be unit magnitude, and

$\nabla f(f,p)$ and $\nabla p(f,p)$ represents the components associated with f and p, respectively, of the gradient $\nabla(f,p)$ of the smooth data fidelity term.

More specifically, some embodiments are based on a realisation of an overall gradient of the data fidelity term in the formulation (6) as described in following proposition:

Proposition:

In some embodiments, the p and f components of the gradient of the data fidelity term in the formulation (6) may, respectively, be expressed as:

$$\nabla_p(f,p) = -\mathrm{diag}(y)^H r, \tag{7}$$

and

$$\nabla_f(f,p) = \mathrm{diag}(u)^H(H^H r + G^H w), \tag{8}$$

where,

r=[H diag(u)f−diag(y)p] is the residual vector,

A=I−G diag(f), and

u and w correspond to solutions of the following linear systems:

$$Au = u_{in}, A^H w = \mathrm{diag}(f)H^H r, \tag{9}$$

linearized around the current estimate of the f.

Proof. The gradient of the data term with respect to p, $\nabla p(f,p)$, may be determined based on matrix derivatives.

Further, with reference to the formulation (6), the derivative with respect to f, $\nabla f(f,p)$, can be expressed as:

$$\nabla_f\left[\frac{1}{2}\left\|[\mathrm{diag}(y), -H\mathrm{diag}(u)]\begin{bmatrix} p \\ f \end{bmatrix}\right\|_2^2\right] = J_f^H r, \tag{10}$$

where J_f represents the Jacobian with respect to f, which can be further expressed as:

$$J_f = \frac{d}{df}(H\mathrm{diag}(u)f). \tag{11}$$

Further, the derivative in the formulation (11) is solved using differentials as:

$$d(H\ \mathrm{diag}(u)f) = H\ \mathrm{diag}(u)df + Hd(\mathrm{diag}(u)f$$
$$= H\ \mathrm{diag}(u)df + H\ \mathrm{diag}(f)du, \tag{12}$$

where some embodiments are based on a realization that u is a function of f and that when taking the differential with respect to only the total field u following relationship is established:

$$d(\mathrm{diag}(u))f = d(\mathrm{diag}(u)f) = d(\mathrm{diag}(f)u) = \mathrm{diag}(f)du.$$

Moreover, with $u=A^{-1}\ u_{in}$, differential of u is expressed as:

$$du = -A^{-1}dAA^{-1}u_{in} = -A^{-1}dAu. \tag{13}$$

Further, differential of A is expressed as:

$$dA = d(I - G\ \mathrm{diag}(f)) = -Gd(\mathrm{diag}(f)), \tag{14}$$

which can be used to arrive at dAu=−Gd(diag(f))u=−G diag(u)df.

By use of all of the differentials, the Jacobian is expressed as:

$$J_f = H\ \mathrm{diag}(u) + H\ \mathrm{diag}(f)A^{-1}G\ \mathrm{diag}(u). \tag{15}$$

Finally, combining (15) and (10), (8) is obtained.

Further, based on the expressions (7) and (8) for the gradient, the processor **204** is configured to compute the required gradient which is used to determine distribution of permittivity of material of the object **106**,**108**.

In accordance with the execution of the PISTA algorithm, the processor **204** solves the multi-variable minimization problem over the unknown phases of the phaseless measurements **216** and the unknown image x of the permittivity of the material of the object **106**,**108**.

Accordingly, the processor **204** determines the distribution of the permittivity of the material of the object **106**,**108** with high resolution and accuracy based on the solution of the multi-variable minimization problem. Further, the processor **204** renders the determined permittivity of the material of the object **106**,**108** via the output interface **222**.

FIG. **3** shows a schematic for workflow of determining the image of the distribution of permittivity of the material of the object **106**,**108** in the scene, according to some embodiments.

The workflow is executed by the processor **204** based on the phaseless measurements of propagation **216**.

The set of instructions, phaseless measurements of propagation **216** of the known incident field u_{in} through the scene and scattered by the material of the object **106**,**108** in the scene, are applied **302**. Further, the processor **204** executes the set of instructions based on the phaseless measurements of the propagation **216** in order to minimize the difference of

a nonlinear function of the known incident field u_{in} and the unknown image x with the product of known magnitudes of the phaseless measurements of the propagation **216** and the unknown phases **304**, optionally with additional constraints and priors on the unknown image and the unknown phases (as described in (6)).

Further, the processor **204** executes the set of program instructions in order to solve the multi-variable minimization problem over the unknown phases of the phaseless measurements of the propagation **216** and unknown image f of the permittivity of the material of the object **106**,**108 306** (as described in description of FIG. **2**B). By the solution of the multi-variable minimization problem, the processor **204** renders the permittivity of the material of the object **106**,**108** via the output interface **222** or the display interface **218 308**. Accordingly, a highly accurate image of the material of the object **106**,**108** is obtained.

FIG. **4**A shows a schematic of a civil infrastructure system to generate a map of non-visible objects in a civil infrastructure, according to some embodiments.

In FIG. **4**A, there is shown a civil infrastructure system **400** in a civil infrastructure **404**, where the civil infrastructure system **400** comprises at least a permittivity sensor **402**, one or more transmitters configured to transmit one or more electromagnetic signals, and one or more receivers configured to receive one or more scattered waves. The permittivity sensor **402** corresponds to the permittivity sensor **200** as described in FIG. **2**A. In FIG. **4**A, there is further shown an underground pipe **406** in mud **408** located underground of the civil infrastructure **404**, where the underground pipe **406** and particles of the mud **406** (such as rocks, soil, water, and the like) may correspond to non-visible objects of the civil infrastructure **404**. Alternatively, the civil infrastructure **404** may include a plurality of pipes located underground as non-visible objects.

In some embodiments, the civil infrastructure system **400** is a moving platform traveling on ground of the civil infrastructure **404**. The civil infrastructure system **400** incidents the electromagnetic signals (such as the known incident field u_{in}) on the ground of the civil infrastructure **404**. When the electromagnetic signals propagate through the ground, the electromagnetic signals are reflected from the non-visible objects (i.e. underground pipe **406** and the particles of the mud **408**).

Based on the reflections (i.e. the one or more scattered waves), the civil infrastructure system **400** detects presence of the non-visible objects located underground of the civil infrastructure **404**.

To that end, the permittivity sensor **402** arranged on the moving platform accepts the reflected electromagnetic signals from the underground pipe **406** and from the particles of the mud **408**. The permittivity sensor **402** further accepts phaseless measurements of the propagated electromagnetic signals with unknown phase (such as the phaseless measurements of propagation **218**).

Further, the permittivity sensor **402** solves a multi-variable minimization problem over unknown phases of the phaseless measurements and unknown image of the permittivity of a material of the underground pipe **406** and the particles of the mud **408**, by minimizing a difference of a nonlinear function of the known incident field and the unknown image with a product of known magnitudes of the phaseless measurements and the unknown phases possibly including additional constraints on the unknown image and the unknown phases as described in description of FIG. **2**A and FIG. **2**B.

Based on the solution of the multi-variable minimization problem, the permittivity sensor **402** determines distribution of permittivity of the material of the underground pipe **406** and the particles of the mud **408**. The permittivity sensor **402** further generates a map **408** of the underground pipe **406** and the particles of the mud **408** based on the permittivity of the underground pipe **406** and renders the map **408** via an output interface (e.g., the output interface **222**). An output of the map **408** of the underground pipe **406** and the particles of mud is illustrated in FIG. **4**B, where the distribution of the permittivity of the material of the non-visible objects (i.e. the underground pipe **406** and the particles of mud **408**) is shown.

FIG. **4**B shows an exemplary output of the map of the non-visible objects, according to some embodiments. In FIG. **4**B, shows is a map **410** that corresponds to the distribution of the permittivity of the material of the underground pipe **406** and the particles of the mud **408**. The map **410** includes an image **412** that corresponds to the particles of the mud **408** and an image **414** that corresponds to the underground pipe **406**. Accordingly, based on the phaseless measurements by means of the permittivity sensor **402** of the civil infrastructure system **400**, the non-visible objects in the civil infrastructure **404** are detected.

FIG. **4**C shows an alternative exemplary output of the map of the non-visible objects, according to some embodiments. In FIG. **4**C, shows a 2-dimensional map **410** that corresponds to the distribution of the permittivity of the material of the underground pipe **406** and the particles of the mud **408** for a cross-section of the pipe. The map **410** includes an image **412** that corresponds to the particles of the mud **408** and an image **414** that corresponds to the underground pipe **406**. Accordingly, based on the phaseless measurements by means of the permittivity sensor **402** of the civil infrastructure system **400**, the non-visible objects in the civil infrastructure **404** are detected.

FIG. **5**A shows a schematic of a civil infrastructure system to generate a map of cavities in non-visible objects in a civil infrastructure, according to some embodiments.

In FIG. **5**A, there is shown a civil infrastructure that comprises objects such as pipes (for example, a pipe **500**). The pipe **500** includes a set of cavities (such as a cavity **502**). In some embodiments, the cavity **502** may be a defect in the pipe **500**. There is further shown a civil infrastructure system **504** that comprises at least a permittivity sensor **506**, one or more transmitters configured to transmit one or more electromagnetic signals, and one or more receivers configured to receive one or more scattered electromagnetic waves. The permittivity sensor **506** corresponds to the permittivity sensor **200** as described in FIG. **2**A and the permittivity sensor **402** as described in FIG. **4**A.

As shown in FIG. **5**A, the civil infrastructure system **504** is a moving platform traveling inside the pipes (i.e. the pipe **500**). As the civil infrastructure system **504** moves inside the pipe **500**, the civil infrastructure system **504** incidents the electromagnetic signals (such as the known incident field u_{in}) on an inside structure of the pipe **500** via the one or more transmitters.

When the electromagnetic signals propagate inside the pipe **500**, the electromagnetic signals are reflected from the inside structure of the pipe **500** and are received by the civil infrastructure system **504** via the one or more receivers. However, a portion of the pipe **500** where the cavity **502** is formed does not reflect back the electromagnetic wave as the incident electromagnetic wave propagates through the cavity **502** and further enters into a space outside the pipe **500**.

Accordingly, the civil infrastructure system **504** does not receive the electromagnetic waves from the cavity **502**.

Based on the reflections of the electromagnetic waves from the pipe **500**, the civil infrastructure system **504** generates a map **508** of permittivity distribution of the inside structure of the pipe **500** by means of the permittivity sensor **506** (as described in description of FIG. **2**B and FIG. **4**A). Such a map is also called as a map of the cavities of the pipes. An output of the map of the cavities (i.e. the map **508**) is shown in FIG. **5**B, where the distribution of the permittivity of the inside structure of the pipe **500** is shown.

FIG. **5**B shows, an exemplary output of the map of cavities of the non-visible objects in the civil infrastructure, according to some embodiments. In FIG. **5**B, there is shown a map **508**, where a part **510** of the map **508** represents the cavity **502**. Accordingly, the civil infrastructure system **504** detects the defects in the objects of the civil infrastructure by use of the permittivity sensor **506**.

FIG. **6** shows a schematic of comparison of experiment results for permittivity distribution of a material of an object using the PISTA algorithm and state of art algorithms with high contrast settings, according to some embodiments.

For instance, an object has a physical size of 15 cm*15 cm with two cylinders of permittivity contrast values 2 and 0.45, respectively, which is illuminated with one or more light signals containing multiple wavelengths (e.g., multiple wavelengths of 6 cm, 7.5 cm, 10 cm, 15 cm, and 30 cm) via a number of transmitters. Further, one or more scattered light signals are received from the object in order to obtain the experiment results.

To that end, the pixel size is set to 0.4688 cm and the number of transmitters is set to 24 with 36 receivers measuring the scattered light signal received from the object. The transmitters and receivers are uniformly placed in a circle of radius 1.67 m around the object. Further, the one or more scattered light signals are processed based on the state of art algorithm (e.g., alternating direction method of multipliers (ADMM)) and the PISTA algorithm, and accordingly the experiment results are obtained. More specifically, phaseless measurements of propagation of the one or more light signals are obtained by a processor (e.g., the processor **204**), where the propagation measurements comprise information of at least the one or more scattered light signals, the one or more light signals incident on the object, or a magnitude of the one or more light signals. Further, the processor executes the set of program instructions to solve the nonlinear image inversion problem based on the propagation measurements as described in description of FIG. **2**A and FIG. **2**B.

Accordingly, an image of the object is reconstructed as the output map **602** and as the output map **604** based on the solution of the nonlinear image inversion problem using the ADMM algorithm and the PISTA algorithm at different contrast settings respectively.

In FIG. **6**, there is shown a set of experiment results in a top row and in a bottom row with high contrast settings, where the high contrast settings are based on setting of a maximum permittivity contrast. More specifically, the top row contains experiment results for the object having maximum permittivity contrast **2** and the image is reconstructed using phaseless measurements of the scattered wave at multiple wavelengths. The bottom row contains experiment results for the object having maximum permittivity contrast **10** while using phaseless measurements of the scattered wave at only one wavelength (i.e., a wavelength of 30 cm).

There is further shown a simulated image **600** of the object in the top row and in the bottom row. Further, there is shown an output map **602** in the top row and in the bottom row, where the output map **602** is an experiment result generated based on the PISTA algorithm. Further, there is shown an output map **604** in the top row and in the bottom row, where the output map **604** is an experiment result generated based on the state of art algorithm ADMM.

Further, as shown in FIG. **6**, reconstruction performance of both approaches (i.e. the ADMM algorithm and the PISTA algorithm) is reasonable for moderate contrast, however the PISTA algorithm visibly outperforms the ADMM algorithm for high contrast settings with only one frequency.

FIG. **7** shows a schematic of comparison of experiment results for permittivity distribution of a material of an object using the PISTA algorithm and state of art algorithms at different frequencies, according to some embodiments.

In FIG. **7**, there is shown experimental measurements for an object FoamDielExt™ from a Fresnel Institute public dataset. For instance, a region of 15 cm×15 cm is considered around an origin where the object FoamDielExt™ is placed. Further, eight transmitters and 360 receivers are placed uniformly in a circle of radius 1.67 m around the origin. The transmitters are turned on one at a time and data from only 241 receivers is used. The remaining 119 receivers closest to the transmitter are kept inactive.

Further, in FIG. **7**, there is shown the object FoamDielExt™ as a ground truth **700** and reconstructed images (i.e. images **702-708**) of the object (i.e. permittivity distribution map) based on the PISTA algorithm and the ADMM algorithm, in a top row and in a bottom row. The images **702** and **706** are based on the PISTA algorithm and the images **704** and **708** are based on the ADMM algorithm. Further, the images **702** and **704** (in the top row) are reconstructed for a single frequency of wavelength 10 cm, and images **704** and **706** (in the bottom row) are reconstructed for multiple frequencies of wavelengths 5 cm, 6 cm, 7.5 cm, 10 cm, and 15 cm at a pixel size of 0.4688 cm, where reconstruction of the images **702-708** of the object is same as described in description of FIG. **2**B, and FIG. **6**.

Further, from FIG. **7**, it is clear that in some situation, the PISTA results in better reconstructions than the ADMM.

The above description provides exemplary embodiments only, and is not intended to limit the scope, applicability, or configuration of the disclosure. Rather, the above description of the exemplary embodiments will provide those skilled in the art with an enabling description for implementing one or more exemplary embodiments. Contemplated are various changes that may be made in the function and arrangement of elements without departing from the spirit and scope of the subject matter disclosed as set forth in the appended claims.

Specific details are given in the above description to provide a thorough understanding of the embodiments. However, if understood by one of ordinary skill in the art the embodiments may be practiced without these specific details. For example, systems, processes, and other elements in the subject matter disclosed may be shown as components in block diagram form in order not to obscure the embodiments in unnecessary detail. In other instances, well-known processes, structures, and techniques may be shown without unnecessary detail in order to avoid obscuring the embodiments. Further, like reference numbers and designations in the various drawings indicated like elements.

Also, individual embodiments may be described as a process which is depicted as a flowchart, a flow diagram, a data flow diagram, a structure diagram, or a block diagram. Although a flowchart may describe the operations as a sequential process, many of the operations may be per-

formed in parallel or concurrently. In addition, the order of the operations may be re-arranged. A process may be terminated when its operations are completed, but may have additional steps not discussed or included in a figure. Furthermore, not all operations in any particularly described process may occur in all embodiments. A process may correspond to a method, a function, a procedure, a subroutine, a subprogram, etc. When a process corresponds to a function, the function's termination can correspond to a return of the function to the calling function or the main function.

Furthermore, embodiments of the subject matter disclosed may be implemented, at least in part, either manually or automatically. Manual or automatic implementations may be executed, or at least assisted, through the use of machines, hardware, software, firmware, middleware, microcode, hardware description languages, or any combination thereof. When implemented in software, firmware, middleware or microcode, the program code or code segments to perform the necessary tasks may be stored in a machine readable medium. A processor(s) may perform the necessary tasks.

Various methods or processes outlined herein may be coded as software that is executable on one or more processors that employ any one of a variety of operating systems or platforms. Additionally, such software may be written using any of a number of suitable programming languages and/or programming or scripting tools, and also may be compiled as executable machine language code or intermediate code that is executed on a framework or virtual machine. Typically, the functionality of the program modules may be combined or distributed as desired in various embodiments.

Embodiments of the present disclosure may be embodied as a method, of which an example has been provided. The acts performed as part of the method may be ordered in any suitable way. Accordingly, embodiments may be constructed in which acts are performed in an order different than illustrated, which may include performing some acts concurrently, even though shown as sequential acts in illustrative embodiments.

Although the present disclosure has been described with reference to certain preferred embodiments, it is to be understood that various other adaptations and modifications can be made within the spirit and scope of the present disclosure. Therefore, it is the aspect of the append claims to cover all such variations and modifications as come within the true spirit and scope of the present disclosure.

We claim:

1. A permittivity sensor for determining an image of a distribution of permittivity of a material of an object in a scene, comprising:

a transmitter configured to propagate a known incident field through the scene;

a receiver configured to accept phaseless measurements of propagation of the known incident field scattered by the material of the object in the scene;

a hardware processor configured to solve a multi-variable minimization problem over unknown phases of the phaseless measurements and unknown image of the permittivity of the material of the object by minimizing a difference of a nonlinear function of the known incident field and the unknown image with a product of known magnitudes of the phaseless measurements and the unknown phases, estimate the permittivity of the material of the object based on the solution of the multi-variable minimization problem, and generate the image of the distribution of permittivity of the material of the object in the scene based on the estimated permittivity; and

a display device configured to render the image of the distribution of permittivity of the material of the object in the scene.

2. The permittivity sensor of claim **1**, wherein the processor is configured to solve the multi-variable minimization problem using a simultaneous multi-variable minimization over both unknowns simultaneously by updating the both unknowns for each iteration.

3. The permittivity sensor of claim **2**, wherein the simultaneous multi-variable minimization uses a multi-variable proximal gradient method.

4. The permittivity sensor of claim **1**, wherein the multi-variable minimization problem further includes additional constraints on the unknown image and the unknown phases.

5. The permittivity sensor of claim **4**, wherein the multi-variable proximal gradient method is implemented using fast iterative shrinkage-thresholding algorithm (FISTA).

6. The permittivity sensor of claim **1**, wherein the processor is configured to solve the multi-variable minimization problem using an alternating minimization.

7. The permittivity sensor of claim **1**, wherein the output interface renders the permittivity of the material of the object to a civil infrastructure system configured to detect at least one of defects of the material of the object, cavities or non-visible objects of the civil infrastructure.

8. The permittivity sensor of claim **7**, wherein the civil infrastructure system is configured to detect the non-visible objects including pipes located underground, and wherein the permittivity sensor is arranged on a moving platform traveling on the ground above the underground pipes, and wherein the civil infrastructure system is configured to generate a map of the underground pipes.

9. The permittivity sensor of claim **7**, wherein the civil infrastructure system is configured to detect the cavities of objects of the civil infrastructure including pipes, and wherein the permittivity sensor is arranged on a moving platform traveling through the pipes, and wherein the civil infrastructure system is configured to generate a map of the cavities of the pipes.

10. The permittivity sensor of claim **1**, wherein the permittivity of the material of the object corresponds to at least one of an internal structure of the object or an outer structure of the object.

11. A robot including the permittivity sensor of claim **1**, the robot comprising:

a motor and wheels for moving the permittivity sensor to the scene.

12. A method for determining an image of a distribution of permittivity of a material of an object in a scene, wherein the method uses a processor coupled with stored instructions implementing the method, wherein the instructions, when executed by the processor carry out steps of the method, comprising:

propagating, using a transmitter, a known incident field through the scene;

accepting, using a receiver, phaseless measurements of propagation of the known incident field scattered by the material of the object in the scene;

solving a multi-variable minimization problem over unknown phases of the phaseless measurements and unknown image of the permittivity of the material of the object by minimizing a difference of a nonlinear function of the known incident field and the unknown

image with a product of known magnitudes of the phaseless measurements and the unknown phases;

estimating the permittivity of the material of the object based on the solution of the multi-variable minimization problem;

generating the image of the distribution of permittivity of the material of the object in the scene based on the estimated permittivity; and

rendering the image of the distribution of permittivity of the material of the object on a display device.

13. The method of claim **12**, wherein the multivariable minimization problem further includes additional constraints on the unknown image and the unknown phases.

* * * * *